

THE UNIVERSITY OF BRITISH COLUMBIA  
DEPARTMENT OF STATISTICS  
TECHNICAL REPORT #270

A review of dynamic duration of load models  
for lumber strength

BY

YONGLIANG ZHAI, CIPRIAN PIRVU,  
NANCY HECKMAN, CONROY LUM, LANG WU,  
JAMES V ZIDEK

November 2012

# A review of dynamic duration of load models for lumber strength

Yongliang Zhai<sup>1</sup>, Ciprian Pirvu<sup>2</sup>, Nancy Heckman<sup>1</sup>, Conroy Lum<sup>2</sup>,  
Lang Wu<sup>1</sup>, James V Zidek<sup>1</sup>

<sup>1</sup> Department of Statistics, University of British Columbia

<sup>2</sup> FPInnovations, Vancouver, BC

Oct 2012

## **Abstract**

The duration of load effect is a distinctive and important characteristic of wood strength. It refers to the fact that wood products can usually sustain a high load for a short time but can also sustain long-term continuous lower loads, albeit with some deformation. Modelling the duration of load effect and testing wood for specific properties of this effect are important in ensuring structural safety of wood construction. Damage accumulation models have been proposed by several researchers to model the duration of load effects. The models assume that damage is accumulated over time according to the load history, and once the accumulated damage reaches a threshold value, the board will break. Different researchers have designed different experiments and proposed different methods for estimating the model parameters.

In this work, we consider several damage accumulation models, with a focus on the U.S. model. We investigate the effects of the distributional assumptions for the models, and propose several methods to estimate parameters in the models. Our proposed methods are evaluated via simulation studies. We apply our methods to a dataset from Foschi and Yao (1986)'s experiments.

# 1 Introduction

The duration of load effect describes the deformation of a product under constant long-term loading, a deformation that can lead to breakage of the product. Models for this effect are usually formulated in terms of the *accumulation of damage*. This report reviews the duration of load effect on wood products and the attempts that have been made to model the accumulated damage resulting from that effect. We begin with a description of the duration of load effect.

Under long-term loading, material such as wood deforms over time, with some of the deformation being permanent. The process of deformation of a material under constant loading is called *creep*.

Duration of load is associated with the creep-rupture behavior that occurs in the third phase of deformation. The magnitude of deformation depends on load level, which is generally controlled by code requirements to ensure an acceptable deformation limit of the structure over time.

Creep and duration of load effects of wood are of critical importance to timber engineering. To account for the duration of load behavior, design codes use adjustment factors recommended for sawn lumber and engineered wood products. The adjustment factors specified for wood products and connectors in the North American wood design standards are based on early damage accumulation models with parameters calibrated to experimental results for dimension lumber (Karacabeyli and Soltis, 1991). An important question is whether the early damage accumulation models apply to the current wood products, especially to the recent generation of composite wood-based products. To accurately model the behavior of these current wood products, the applicability of accumulation of damage models must be studied and, if needed, the models and/or parameters must be updated. Statistical approaches are crucial in addressing this issue.

The duration of load test is a constant load test at a load level  $\tau_a$  defined in a ramp load test. Figure 1 illustrates the load history in the ramp load test and in the constant load test. Let  $\tau(t)$  denote the load at time  $t$ . In the ramp load test with rate  $k$ , the applied load is linear in  $t$ , that is  $\tau(t) = kt$ . In the ramp load test, the breaking time is  $T_s$ , and the breaking load is  $\tau(T_s) = kT_s$ . Figure 2 provides a schematic of the duration of load test set up.

In the constant load test, the load first increases linearly at constant rate  $k$  until a predetermined time  $T_0$ , similar to the initial period of the ramp load test, and then the load remains constant during the rest of time (see

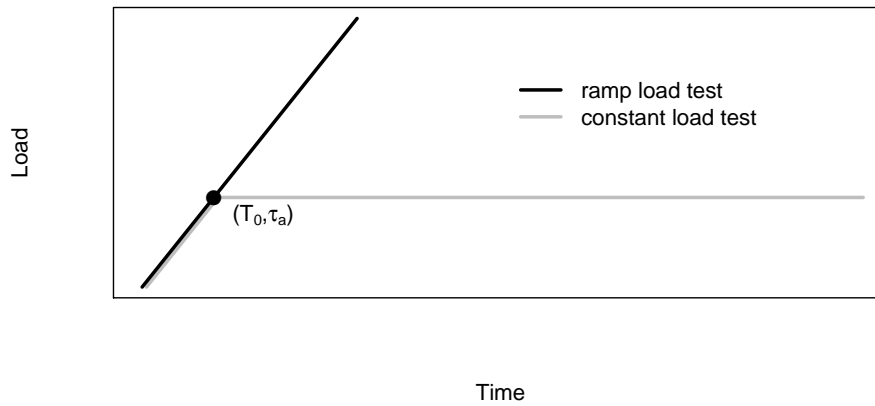


Figure 1: An illustration of the ramp load test and the constant load test. In the ramp load test, the load increases linearly over time until the wood specimen fails. In the constant load test, the load first increases linearly until it reaches a pre-determined load  $\tau_a$  at time  $T_0$  and then stays constant thereafter until the specimen fails or the experiment ends.

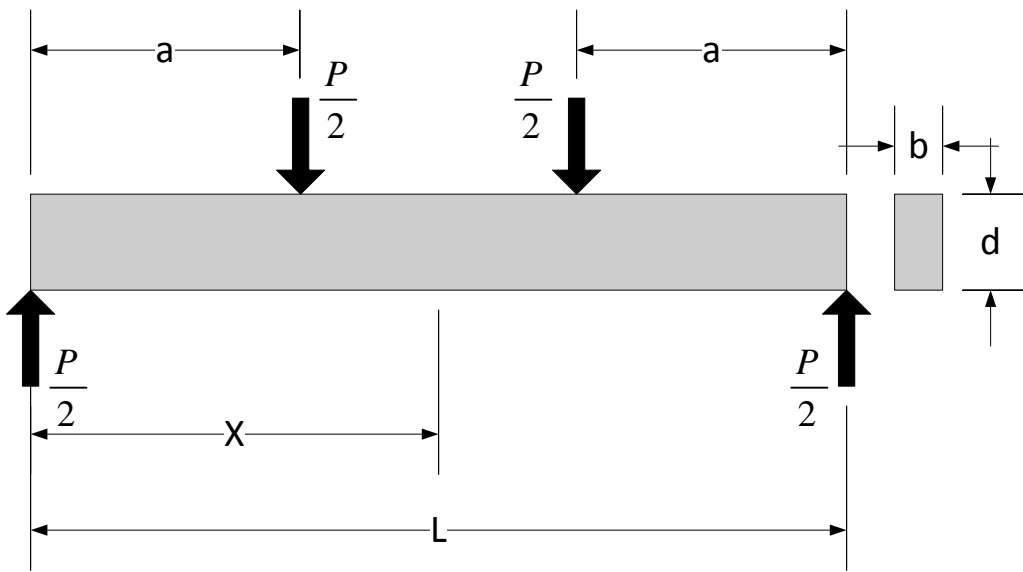


Figure 2: Diagram showing how the loads are applied in the bending tests. In the diagram,  $a$  = distance from reaction to nearest load point (or, half of shear span) (mm/in),  $P$  = bending load applied to specimen (N/lbf),  $b$  = specimen width (mm/in),  $d$  = specimen depth (mm/in),  $L$  = span of specimen (mm/in), and  $X$  = half of span (mm/in).

Figure 1). That is

$$\tau(t) = \begin{cases} kt & \text{for } 0 \leq t \leq T_0, \\ kT_0 & \text{for } t > T_0. \end{cases}$$

The pre-determined load level  $kT_0$  is denoted by  $\tau_a$ , i.e.,  $\tau_a = kT_0$ . The load level  $\tau_a$  is usually set at a certain percentile of the empirical distribution of the short-term strength of the wood specimens tested during a ramp load test with load equal to  $kt$ , the same value of  $k$  as in the constant load test. The first part of the constant load test (i.e.,  $\tau(t) = kt$  when  $0 \leq t \leq T_0$ ) is called the *ramp loading part of the constant load test* and the second part of the constant load test (i.e.,  $\tau(t) = \tau_a$  when  $t > T_0$ ) is called the *constant loading part of the constant load test* (see Figure 1).

There are also other ways to set up duration of load experiments. The most popular one in industry can be summarized in three phases of deformation under constant loading:

1. an initial deformation triggered by the application of the constant load
2. a secondary deformation entirely dependent on the load level applied;
3. a third deformation characterized by a spike in deformation until failure occurs.

In this paper, we focus on the experiments set up shown in Figure 1.

The duration of load effect is usually modelled in terms of the *accumulation of damage*. Proposing a model for damage accumulation based on physical laws is difficult, since our knowledge of material behavior at the microscopic level where the deterioration happens is generally incomplete. As an alternative, damage accumulation models have been proposed based instead on a combination of our incomplete understanding of the phenomena at the macroscopic level and examination of experimental data (Yao, 1987). In an accumulation of damage model, a wood specimen accumulates damage depending on some load  $\tau$  that may vary over time. The damage accumulated by time  $t$  is denoted  $\alpha(t)$  with, by convention,  $\alpha(0) = 0$  and  $\alpha(T) = 1$ , where  $T$  is the *breaking time* of the specimen;  $\alpha$  is a non-decreasing function of  $t$ . The accumulated damage process cannot be observed, but it may be inferred based on the observed breaking times. The advantage of damage accumulation models is that they may facilitate the prediction of damage

produced by an arbitrary load sequence, which may be useful in reliability tests.

All damage accumulation models we review are based on the following differential equation:

$$\frac{d\alpha(t)}{dt} = f(\alpha(t), \tau(t), \theta), \quad (1)$$

where  $f$  is a known function,  $\tau(t)$  is the known load at time  $t$ , and  $\theta$  is a vector of parameters, usually unknown.

The short term strength  $\tau_s$  is often included as an argument of  $f$  in equation (1), in the form of  $\sigma(t) = \tau(t)/\tau_s$ . However, authors define  $\tau_s$  in different ways. Gerhards and Link (1987) treat  $\tau_s$  as a specimen dependent random parameter with an assumed distribution and do not define  $\tau_s$  in terms of any breaking time or load pattern. Foschi and Yao (1986) also treat  $\tau_s$  as a specimen dependent parameter, but define  $\tau_s$  as the breaking load  $\tau(T_s)$  in the ramp load test, when the loading rate  $k$  is set so that the mean breaking time is expected to be around one minute. Different definitions of  $\tau_s$  lead to different damage accumulation models. We mostly focus on the model of Foschi and Yao (1986) in this report.

In the literature, the parameter vector  $\theta$  is often treated as a constant vector, depending on the type of wood specimen but constant among specimens of the same type. However, this implies that all specimens of the same type, when subjected to the same load, have the same breaking time  $T$ , since, for a fixed  $\theta$  and load, at most one value of  $T$  can satisfy  $\alpha(T) = 1$ . Clearly this is not realistic, as breaking times do vary from specimen to specimen. A perhaps more realistic approach is to treat the parameters  $\theta$  as random effects, which vary from specimen to specimen. This approach was taken by Foschi and Yao (1982, 1986), as well as Gerhards and Link (1987).

Authors have proposed various parameter estimation methods from breaking times  $T_s$ 's in the ramp load test and/or breaking times  $T_c$ 's in the constant load test. However, the estimation of parameters has been done in an ad hoc way with no statistical principles, thereby leaving room for possible improvement. These authors have not discussed the distributions of the breaking times. Also, no one has considered random effects in the U.S. model.

In this paper, we review several damage accumulation models in the literature: the Madison Curve model, the U.S. model, and the Canadian model. We derive the solutions or the approximate solutions they imply for the breaking time  $T_s$  in the ramp load test and the breaking time  $T_c$  in the constant load test for the U.S. model and the Canadian model. We also review the

parameter estimation methods found in the literature. Finally, we discuss the problem of scale for some models.

Section 5 gives some concluding remarks, which in particular argue that the review presented in this paper is a timely one.

## 2 Damage models, scales and units of measurement

This section reviews some fundamental issues that arise in modeling the accumulated damage in a randomly selected wood specimen under a specified stress loading, issues that have not always been recognized in developing those models. No model that describes a physical phenomenon should depend on the units in which those properties will be measured. A first step in meeting this requirement entails “non-dimensionalizing” the model, that is, entails choosing the scales of the quantities involved in the models including the baseline units for their scales. Those quantities then become unitless numbers of the baseline units.

In accumulated damage models time is such a quantity. Depending on the nature of the applied stress load, the natural scale could be anything from seconds to weeks. Years, although a seemingly natural scale for long term load effects, would not be appropriate since the length of a year is not well-defined. Minutes might be appropriate for modelling the duration of load effect in a proof loading ramp load test. In any case time would be expressed as a unitless number of baseline units on the designated scale.

Non-dimensionalizing models can have a number of benefits such as simplifying dynamic differential equation models. Of more direct relevance to the topic of this paper, transcendental functions such as  $\log x$  and  $\exp(x)$  can be used meaningfully. By their definition such functions as well as their arguments must in principle be unitless (Matta et al. 2011), for otherwise models involving them would be meaningless. Violations of this principle in damage modeling can be seen in Cai et al. (2000; see their Figure 1 for example), Foschi and Barrett (1982; see their Figure 2 for example) and Gerhards (1988; see Equation (1) for example). The deficiency in these models can be rectified by non-dimensionalizing them although thought would need to be given as to how best to do that. In any case, in the review of the theory that follows we explicitly describe how this change can be made.

### 3 Stochastic duration of load models

This section reviews some well-known damage accumulation models, the Madison Curve model, the U.S. model and the Canadian model along with its predecessors. Note that, for damage accumulation models, the accumulated damage  $\alpha(t)$  cannot be observed. Instead we only observe the failure time  $T_s$  and/or  $T_c$ . Therefore, we focus on the solutions for  $T_s$  and  $T_c$  implied by the damage accumulation models.

We review the solutions for the breaking time  $T_s$  in the ramp load test and the breaking time  $T_c$  in the constant load test for the U.S. model. We discuss both Gerhards and Link's approach (1987) and Foschi and Yao's approach (1986) for the U.S. model.

We review the approximate solutions of the breaking time  $T_s$  in the ramp load test and the breaking time  $T_c$  in the constant load test proposed by Foschi and Yao (1986) for the Canadian model. We discuss Foschi and Yao's method for parameter estimation in the Canadian model.

We discuss the problem of scale, which is a common problem in damage accumulation models. We propose a method to revise the damage accumulation models to eliminate the problem of scale.

Table 1 summarizes commonly used notation and their definitions.

Sections 3.1 through 3.3 present details of some damage accumulation models. Section 3.1 is a brief review of a damage accumulation model based on the Madison Curve proposed by Hendrickson et al. (1987). Section 3.2 contains a review of an exponential damage accumulation model (the U.S. model) proposed by Gerhards (1979). Section 3.3 contains a review of a sequence of models including the Canadian model proposed by Foschi and his collaborators. In this report, we will focus on the U.S. model and the Canadian model. Section 3.4 discusses revisions of the damage accumulation models to eliminate scale.

#### 3.1 Madison curve

In North America, the duration of load effect was initially discussed in Wood's (1951) work. Unfortunately, this work is unavailable and we rely on Gerhards (1977) for its contents. According to Gerhards, Wood conditioned small clear bending specimens of dried Douglas-fir to achieve 6% and 12% moisture contents and then subjected them to constant load levels ranging from 60% to 95% of their short-term strength. Wood's data from the constant load

Notations	Definitions	Comments
$\alpha(t)$	damage accumulated by time $t$	$0 \leq \alpha(t) \leq 1$
$T_s$	breaking time in the ramp load test	$\alpha(T_s) = 1$
$T_c$	breaking time in the constant load test	$\alpha(T_c) = 1$
$\tau(t)$	applied load (applied stress) at time $t$	-
$\tau_s$	short term strength	-
$\sigma(t)$	applied load ratio at time $t$	$\sigma(t) = \tau(t)/\tau_s$
$\sigma_0$	threshold load ratio	$0 \leq \sigma_0 \leq 1$

Table 1: Commonly used notation for damage accumulation models.

test are shown in Figure 3, but it is not clear whether that figure presents all data from both moisture contents.

According to Gerhards (1977), Wood proposed a hyperbolic empirical model:

$$\sigma = a + bT^c, \quad (2)$$

where  $\sigma$  is the applied load ratio,  $T$  is the breaking time, and  $a, b$  and  $c$  are unknown parameters. Based on the partial data of Wood's constant load test and the results of a ramp load test by Markwardt and Liska (1948), Wood estimated the parameters as:  $\hat{a} = 18.03$ ,  $\hat{b} = 108.4$  and  $\hat{c} = -0.04635$ . The equation (2) with Wood's estimates is called the Madison Curve. Gerhards (1977) did not mention which loading rate was used to reach the constant load in Wood's experiments nor which moisture content level was used to obtain the Madison Curve. Wood's original plot of the Madison Curve is shown in Figure 4.

According to Gerhards (1977), breaking times of various wood products have been modelled based on the Madison Curve. The validity of the Madison Curve has been questioned for a long time. However, due to its simplicity, the Madison Curve is still used today as the basis for the National Design Specification for Wood Construction (NDS) by the American Wood Council.

Based on the Madison Curve, a damage accumulation model for the duration of load effect was developed by Hendrickson et al. (1987):

$$\frac{d\alpha(t)}{dt} = a\{\sigma(t) - \sigma_0\}_+^b, \quad (3)$$

where  $a, b$  and  $\sigma_0$  are model parameters. Here,  $(\sigma - \sigma_0)_+ = \max\{(\sigma - \sigma_0), 0\}$ , which means that the damage will only accumulate when the applied load ratio is larger than the threshold load ratio, i.e.,  $\sigma(t) > \sigma_0$ .

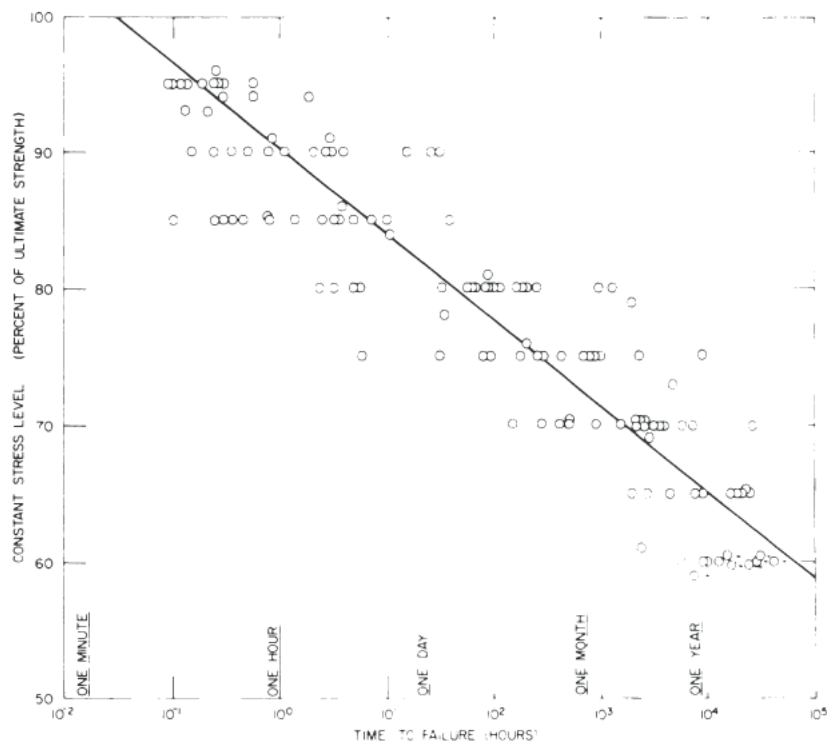


Figure 3: Data from constant load tests by Wood (1951), reproduced from Gerhards (1977). The  $x$ -axis is the breaking time  $T$  in hours and the  $y$ -axis is the applied load ratio  $\sigma$  in percentage.

It is easy to show that, if for all  $t$ ,  $\sigma(t) = \sigma_a > \sigma_0$ , then for (3), the solution for  $T$  with  $\alpha(T) = 1$  satisfies

$$\sigma_a = \sigma_0 + (1/a)^{1/b} T^{-1/b},$$

which has the same form of the Madison Curve. Wang (2009) called model (3) the model derived from the Madison Curve. We call model (3) the Madison Curve model.

### 3.2 The U.S. model

The U.S. model, also called the *exponential damage rate model (EDRM)*, was proposed by Gerhards (1979). Based on the assumption that the accumu-

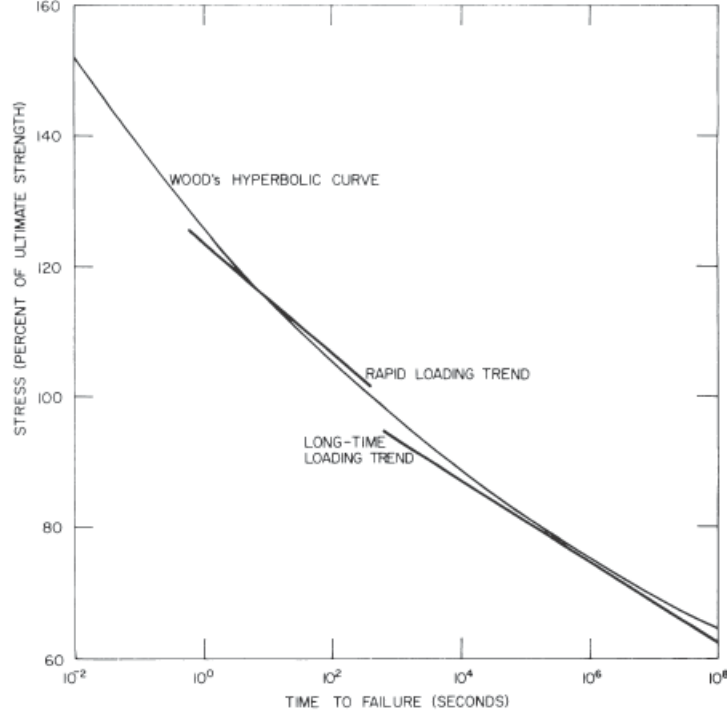


Figure 4: Madison Curve with ramp loading test trends and constant loading test trends by Wood (1951), reproduced from Gerhards (1977). The  $x$ -axis is the breaking time  $T$  in seconds and the  $y$ -axis is the applied load ratio  $\sigma$  in percentage.

lated damage is an exponential function of the applied load ratio, Gerhards proposed the following model:

$$\frac{d\alpha(t)}{dt} = \exp \{-a + b\sigma(t)\}, \quad (4)$$

where  $a$  and  $b$  are model parameters. Here,  $b > 0$ . Some authors consider the parameters are fixed while others consider the parameters are random.

The U.S. model has been discussed in Gerhard and Link (1987) as well as Foschi and Yao (1986). Although these represent the U.S. model in the same form in their papers, they actually discuss two different models based on their different definitions of the short term strength  $\tau_s$ .

Gerhards and Link treat the short term strength  $\tau_s$  as a wood specimen dependent parameter and assume that  $\tau_s$  follows a log-normal distribution with median  $\tau_m$ . They do not define  $\tau_s$  in terms of any breaking time or load pattern.

Foschi and Yao treat the U.S. model in a different way. They also consider the short term strength  $\tau_s$  as a specimen dependent parameter, but they further define  $\tau_s$  as the breaking load  $\tau(T_s)$  of the ramp load test when the loading rate  $k$  is set so that the mean breaking time is expected to be around one minute.

In both approaches, the breaking time is random since the short term strength  $\tau_s$  is random.

The Gerhards-Link and Foschi-Yao analyses had some common calculation steps and some differences in their analysis. The specific calculations are given in the next three subsections.

### Common steps in the Gerhards-Link and Foschi-Yao analyses

Although Gerhards and Link and Foschi and Yao define the U.S. model in different ways, they still go through some common steps to calculate the solution for the breaking time  $T_s$  in the ramp load test and the solution for the breaking time  $T_c$  in the constant load test. The integration of the differential equation is exactly the same in their analysis, but the solutions appear in different forms due to their different definitions of the short term strength  $\tau_s$  and their different notation for other parameters.

In this section, we review the common steps of their calculations for solving the U.S. model for  $T_s$  and  $T_c$ .

For the ramp load test,  $\sigma(t) = kt/\tau_s$ , we can integrate (4) to get  $\alpha(t)$ :

$$\alpha(t) = \int_0^t \exp(-a + bks/\tau_s) ds = \frac{\tau_s}{bk} \{\exp(-a + bkt/\tau_s) - \exp(-a)\}. \quad (5)$$

Based on the fact that  $\alpha(T_s) = 1$ , we get the equation:

$$\frac{\tau_s}{bk} \{\exp(-a + bkT_s/\tau_s) - \exp(-a)\} = 1. \quad (6)$$

Gerhards and Link solve the above equation (6) for  $T_s$  in terms of  $a, b, k$  and  $\tau_s$ . Foschi and Yao solve the above equation (6) for  $T_s$  with another condition that  $\tau_s = kT_s$ , so Foschi and Yao's solution of  $T_s$  does not contain  $\tau_s$ . The exact forms of the solutions are contained in the next two subsections.

For the constant load test, as we discussed in the Introduction, the applied load is  $\tau(t) = kt$  in the ramp loading part for  $0 \leq t \leq T_0$  and then  $\tau(t) = kT_0 = \tau_a$  in the constant loading part for  $t > T_0$ . If  $T_s \leq T_0$  or equivalently, if  $\alpha(T_0) \geq 1$ , then the wood specimen breaks during ramp loading.

For the case that  $T_s > T_0$ , the breaking time  $T_c$  will depend on the damage accumulated during the ramp loading part and during the constant loading part. The damage accumulated during the ramp loading part can be calculated from (5):

$$\begin{aligned}\alpha_0 = \alpha(T_0) &= \frac{\tau_s}{bk} \{ \exp(-a + bkT_0/\tau_s) - \exp(-a) \} \\ &= \frac{\tau_s}{bk} \{ \exp(-a + b\tau_a/\tau_s) - \exp(-a) \}.\end{aligned}\quad (7)$$

In the constant loading part of the constant load test,  $\tau(t) = \tau_a$ , so we can integrate (4) from  $T_0$  to find the damage accumulated during the constant loading part, and then find the total damage accumulated by time  $t > T_0$ :

$$\alpha(t) = \alpha_0 + \int_{T_0}^t \exp(-a + b\tau_a/\tau_s) ds = \alpha_0 + (t - T_0) \exp(-a + b\tau_a/\tau_s), \text{ for } t > T_0.\quad (8)$$

Setting  $\alpha(T_c)$  in (8) equal to 1 and solving for  $T_c$  yields

$$T_c = T_0 + (1 - \alpha_0) / \exp(-a + b\tau_a/\tau_s)\quad (9)$$

if  $T_c > T_0$ .

The above steps for finding  $T_c$  are the same as in Gerhards and Link's analysis as well as Foschi and Yao's analysis. Gerhards and Link solve for  $T_c$  as in (9) in terms of  $a, b, k, T_0$  and  $\tau_s$ . Foschi and Yao solve for  $\tau_s$  in terms of  $a$  and  $b$ , and substitute the result into (9), so Foschi and Yao's solution of  $T_c$  does not contain  $\tau_s$ . The exact forms of the solutions are contained in the next two subsections.

### **Solutions for $T_s$ and $T_c$ from Gerhards and Link's (1987) approach**

Gerhards and Link (1987) assume that  $\tau_s$  is log-normally distributed and expressed  $\tau_s$  as follows:

$$\tau_s = \tau_m \exp(wR)$$

where  $\tau_m$  is the median short term strength,  $w$  is a (unitless) scale parameter and  $R$  is a standard normal random effect.

To get their forms of  $T_s$ ,  $\alpha_0$  and  $T_c$ , let  $B = b/\tau_s = b/\{\tau_m \exp(wR)\}$ . Then we can solve for the breaking time  $T_s$  in the ramp load test from (6):

$$T_s = \frac{\ln \{Bk \exp(a) + 1\}}{Bk}. \quad (10)$$

Note that, here,  $T_s \neq \tau_s/k$ .

Substituting  $B$  for  $b/\tau_s$  in (7), we can write  $\alpha_0$  as

$$\alpha_0 = \frac{1}{Bk} \{\exp(-a + B\tau_a) - \exp(-a)\}. \quad (11)$$

Substituting  $B$  for  $b/\tau_s$  and substituting  $\alpha_0$  from (11) in (9), we can write  $T_c$  in the U.S. model as:

$$T_c = \begin{cases} \frac{\ln \{Bk \exp(a) + 1\}}{Bk}, & \text{if } \frac{\ln \{Bk \exp(a) + 1\}}{Bk} \leq T_0, \\ T_0 - \frac{1}{Bk} + \exp(-B\tau_a) \left\{ \frac{1}{Bk} + \exp(a) \right\}, & \text{if } \frac{\ln \{Bk \exp(a) + 1\}}{Bk} > T_0. \end{cases} \quad (12)$$

### Solutions for $T_s$ and $T_c$ from Foschi and Yao's (1986) approach

Foschi and Yao (1986) define the short term strength of a wood specimen as its breaking strength in the ramp load test with the ramp loading rate  $k$  set so that the mean breaking time is around one minute. In other words, they solve for  $\tau_s$  from  $\tau_s = \tau(T_s) = kT_s$ .

For the ramp load test, replacing  $\tau_s$  by  $kT_s$  in (6), we can solve for the breaking time  $T_s$  in the ramp load test:

$$T_s = \frac{\exp(a)b}{\exp(b) - 1} \equiv Ab \quad (13)$$

where  $A \equiv \exp(a)/\{\exp(b) - 1\}$ .

Noticing the fact that  $\tau_s = kT_s$ , (13) is equivalent to:

$$\tau_s = \frac{\exp(a)bk}{\exp(b) - 1} = Abk. \quad (14)$$

Substituting  $\tau_s$  from (14) in (7) and (9), we can write the solution for  $T_c$  in terms of the model parameters  $A$  and  $b$ :

$$T_c = \begin{cases} Ab, & \text{if } Ab \leq T_0, \\ T_0 + A \{\exp(b - T_0/A) - 1\}, & \text{if } Ab > T_0. \end{cases}$$

### 3.3 The Canadian model and its predecessors

Foschi and his collaborators proposed three models: Model I in Barrett and Foschi (1978), Model II in Barrett and Foschi (1978, 1982) and the Canadian Model in Foschi and Yao (1986).

Model I is a generalization of the Madison Curve model, and is given by

$$\frac{d\alpha(t)}{dt} = a\{\sigma(t) - \sigma_0\}_+^b \alpha^c(t), \quad (15)$$

where  $a, b, c$  and  $\sigma_0$  are model parameters.

In Model I, the damage will accumulate only when  $\tau(t)/\tau_s - \sigma_0 > 0$ . For the ramp load test with  $\tau(t) = kt$ , this means that damage can only accumulate at time  $t$  bigger than  $t_0 = \sigma_0\tau_s/k$ .

Barrett and Foschi's Model I takes the current damage status  $\alpha(t)$  into consideration if  $c \neq 0$ . The current damage status appears in the model as a multiplier. If  $c = 0$ , Barrett and Foschi Model I reduces exactly to the Madison Curve model.

Model II uses an additive model to include the current damage status. The model is given by

$$\frac{d\alpha(t)}{dt} = a\{\sigma(t) - \sigma_0\}_+^b + c\alpha(t), \quad (16)$$

where  $a, b, c$  and  $\sigma_0$  are random model parameters. Again, if  $c = 0$ , then Model II reduces to the Madison Curve model.

In Model II, the damage will accumulate if either  $\tau(t)/\tau_s - \sigma_0 > 0$  or  $\alpha(t) > 0$ . If  $\tau(t)$  is non-decreasing, as in the ramp load test and the constant load test, the damage will only accumulate when  $\tau(t)/\tau_s - \sigma_0 > 0$ .

Barrett and Foschi (1982) conducted an experiment on western hemlock lumber with an approximately 10% moisture content. From these data, they estimate the parameters in (16) as  $\hat{a} = 0.721568 \times 10^{-14} \text{ hour}^{-1}$ ;  $\hat{b} = 34.0$ ;  $\hat{c} = 0.150 \times 10^{-2} \text{ hour}^{-1}$  and  $\hat{\sigma}_0 = 0.5$ .

Foschi and Yao (1986) find that inclusion of the second term of Barrett and Foschi's Model II leads to some unreasonable results. For example, if some damage was accumulated before some time  $t_0$  (e.g., if  $\alpha(t_0) = 0.5$ ) and the load was quite small after  $t_0$  (e.g., if  $\sigma(t) = 0.01$  for  $t \geq t_0$ ), the damage would still increase exponentially according to model (16) since the second term in (16) is dominant. However, in practice the damage should not increase exponentially in this case. To correct this problem, Foschi and Yao (1986) propose a third model which is called the Foschi and Yao model or the *Canadian model*:

$$\frac{d\alpha(t)}{dt} = a\{\tau(t) - \sigma_0\tau_s\}_+^b + c\{\tau(t) - \sigma_0\tau_s\}_+^n\alpha(t), \quad (17)$$

where  $a, b, c, n$  and  $\sigma_0$  are model parameters. This model is called the Canadian model since it is the national standard of Canada.

In the Canadian model, the damage will accumulate only when  $\tau(t)/\tau_s - \sigma_0 > 0$ .

Foschi and Yao (1986) assume that the parameters  $a, b, c, n, \sigma_0$  and  $\tau_s$  in the Canadian model are all random effects, which means that  $a, b, c, n, \sigma_0$  and  $\tau_s$  vary from specimen to specimen. There is a dependency among these random effects. In practice,  $a$  can be solved in terms of the others. For all boards of one type under the same conditions, the vector  $(a, b, c, n, \sigma_0, \tau_s)$  follows the same distribution, no matter what the load pattern is. But for specimens of different types or specimens of one type under different conditions such as differing moisture contents, the vector  $(a, b, c, n, \sigma_0, \tau_s)$  may follow a different distribution.

### Solutions for $T_s$ and $T_c$

To get a closed form solution for the breaking time  $T_s$  in the ramp load test, Foschi and Yao (1986) disregarded the second term of the differential equation in (17) and obtained the following simplified model:

$$\frac{d\alpha(t)}{dt} \approx a\{\tau(t) - \sigma_0\tau_s\}_+^b. \quad (18)$$

We can solve for  $\alpha(t)$  explicitly in model (18) for the ramp load test with  $\tau(t) = kt$ , and based on the fact that  $\alpha(t_0) = 0$ :

$$\alpha(t) \approx \int_{t_0}^t a(ks - \sigma_0\tau_s)_+^b ds = \frac{a}{k(b+1)}(kt - \sigma_0\tau_s)_+^{b+1}. \quad (19)$$

The model in (18) is over-parameterized, so Foschi and Yao use (19) to solve for  $a$  in terms of the other specimen-specific parameters. Specifically, they set  $\alpha(T_s) = 1$  and solve (19) for  $a$ , yielding

$$a \approx \frac{k(b+1)}{\{\tau_s(1-\sigma_0)\}^{b+1}}. \quad (20)$$

By replacing  $\tau_s$  with  $kT_s$ , an equivalent expression of the approximation (20) yields:

$$T_s \approx \frac{\{k(b+1)/a\}^{1/(b+1)}}{k(1-\sigma_0)}. \quad (21)$$

In the constant load test, the applied load is  $\tau(t) = kt$  in the ramp loading part for  $0 \leq t \leq T_0$  and then  $\tau(t) = \tau_a$  in the constant loading part for  $t > T_0$ . As we discussed in Section 3.2, if  $T_s \leq T_0$  or equivalently, if  $\alpha(T_0) \geq 1$ , then the specimen breaks during ramp loading.

For the case that  $T_s > T_0$ , Foschi and Yao propose an approximate method to find  $T_c$ , the breaking time during constant loading.

First, they use the integration (19) of the approximate model (18) to calculate  $\alpha_0$ , the approximate accumulated damage during the ramp loading part of the constant load test:

$$\alpha_0 = \alpha(T_0) \approx \frac{a}{k(b+1)}(kT_0 - \sigma_0\tau_s)^{b+1} = \frac{a}{k(b+1)}(\tau_a - \sigma_0\tau_s)^{b+1}. \quad (22)$$

Substituting (20) into (22) gives an approximation for  $\alpha_0$ :

$$\alpha_0 \approx \left( \frac{\tau_a - \sigma_0\tau_s}{\tau_s - \sigma_0\tau_s} \right)^{b+1}. \quad (23)$$

Second, they solve for  $\alpha(t) - \alpha(T_0)$ ,  $t > T_0$  by integrating the full Canadian model (17) for the constant loading part of the constant load test. The accumulated damage at time  $t \geq T_0$  is given by

$$\begin{aligned} \alpha(t) &= \alpha_0 + \int_{T_0}^t d\alpha(s) \\ &= \{\alpha_0 + (a/c)(\tau_a - \sigma_0\tau_s)^{b-n}\} \exp\{c(\tau_a - \sigma_0\tau_s)^n(t - T_0)\} - (a/c)(\tau_a - \sigma_0\tau_s)^{b-n}. \end{aligned}$$

They then find the breaking time  $T_c$  for the constant loading part of the constant load test by solving  $\alpha(T_c) = 1$ , and obtained:

$$T_c = T_0 + \frac{1}{c(\tau_a - \sigma_0\tau_s)^n} \ln \left\{ \frac{1 + (a/c)(\tau_a - \sigma_0\tau_s)^{b-n}}{\alpha_0 + (a/c)(\tau_a - \sigma_0\tau_s)^{b-n}} \right\}. \quad (24)$$

To sum up, Foschi and Yao give an approximate solution for the breaking time  $T_c$  in the Canadian model:

$$T_c \approx \begin{cases} \frac{\{k(b+1)/a\}^{1/(b+1)}}{k(1-\sigma_0)}, & \text{if } \frac{\{k(b+1)/a\}^{1/(b+1)}}{k(1-\sigma_0)} \leq T_0, \\ T_0 + \frac{1}{c(\tau_a - \sigma_0\tau_s)^n} \ln \left\{ \frac{1 + (a/c)(\tau_a - \sigma_0\tau_s)^{b-n}}{\alpha_0 + (a/c)(\tau_a - \sigma_0\tau_s)^{b-n}} \right\}, \\ \text{if } \frac{\{k(b+1)/a\}^{1/(b+1)}}{k(1-\sigma_0)} > T_0, \end{cases} \quad (25)$$

with  $a$  approximated as in (20) and  $\alpha_0$  approximated as in (23).

### Parameter estimation

Foschi and Yao (1986) proposed a criterion to estimate parameters in the Canadian model. They treated  $b, c, n$  and  $\sigma_0$  as independent random effects which follow log-normal distributions with means  $\mu_b, \mu_c, \mu_n$  and  $\mu_{\sigma_0}$  and standard deviations  $\sigma_b, \sigma_c, \sigma_n$  and  $\sigma_{\sigma_0}$  respectively. They treated  $\tau_s$  as a random effect, which is independent of  $b, c, n$  and  $\sigma_0$ , with a distribution equal to the empirical distribution of the short term strength of the boards from the one minute ramp load test. They treated  $a$  as another random effect, which can be solved from others.

Let  $\phi = (\mu_b, \mu_c, \mu_n, \mu_{\sigma_0}, \sigma_b, \sigma_c, \sigma_n, \sigma_{\sigma_0})$ , which is the vector of parameters to be estimated. Foschi and Yao used a numerical algorithm to find a value of  $\phi$  to minimize a simulation-based function. The authors did not define a probability model based function to minimize, but we see that their method can be defined as minimizing an approximation to a function  $\psi$ . To define  $\psi$ , let  $T_{c(1)}, T_{c(2)}, \dots, T_{c(N)}$  be the order statistics of the observed breaking times in the constant load test and let  $F = F(\cdot; \phi)$  be the cumulative distribution function of the breaking times assuming that the Canadian model holds, with parameters equal to  $\phi$ . Then

$$\psi(\phi) = \sum_{j=1}^N \{1 - F^{-1}(j/N; \phi)/T_{c(j)}\}^2. \quad (26)$$

Foschi and Yao minimized an approximation of (26) via a Newton Raphson algorithm, an iterative method which requires calculation of  $F(\cdot; \phi)$  evaluated at the current values of  $\phi$ , along with calculation of all partial derivatives of  $F(\cdot; \phi)$  with respect to  $\phi$ . To carry out this algorithm, they approximated  $F$  by simulating breaking times with distribution  $F(\cdot; \phi)$ . The approximation of  $F$ , which we denote by  $\widehat{F}$ , is simply the empirical distribution function of the simulated breaking times. For derivative approximation, they simply calculated the change in  $\widehat{F}$  over the change in one element of  $\phi$  when the others are fixed. For instance, the partial derivative of  $F$  at  $\phi$  with respect to  $\mu_b$  was approximated by  $\{\widehat{F}(\cdot; \phi_1) - \widehat{F}(\cdot; \phi_2)\}/(0.002\mu_b)$ , where  $\phi_1 = (\mu_b + 0.001\mu_b, \mu_c, \mu_n, \mu_{\sigma_0}, \sigma_b, \sigma_c, \sigma_n, \sigma_{\sigma_0})$  and  $\phi_2 = (\mu_b - 0.001\mu_b, \mu_c, \mu_n, \mu_{\sigma_0}, \sigma_b, \sigma_c, \sigma_n, \sigma_{\sigma_0})$ .

Foschi and Yao (1986) obtained the following estimates: the means of  $b, c, n$  and  $\sigma_0$  are estimated by 35.204,  $0.1559 \times 10^{-6}$ , 1.429 and 0.578 respectively and the standard deviations of  $b, c, n$  and  $\sigma_0$  are estimated by 6.589,  $0.9621 \times 10^{-7}$ , 0.139 and 0.163 respectively. They did not report the units of the parameters in their paper. We should be aware that these are estimates of the means and variances of the log-normal distributed random effects, but not the parameters we usually use to characterize log-normal distributions.

Foschi and Yao's approach to parameter estimation is problematic. The range of  $\sigma_0$  under the log-normal assumption is not the same as the range of  $\sigma_0$  from the experimental perspective. From the experimental perspective, if  $\sigma(t) = \tau(t)/\tau_s = 1$ , i.e., if the applied load equals the short-term strength, the wood specimen will break for sure. This implies  $(1 - \sigma_0)_+ > 0$  and yields  $\sigma_0 < 1$ . However, the probability of getting a random sample larger than 1 from the log-normal distribution with mean 0.578 and standard deviation 0.163 is 0.017, which is not negligible.

### 3.4 The problem of scale

In the previous studies, researchers measured the breaking times in different units of measurement and estimated the parameters in different units of measurement. Gerhards and Link (1987) measured the breaking times in minutes and estimated  $a$  and  $b$  with a unit of  $\log(\text{minute}^{-1})$ , while Foschi and Yao (1986) measured the breaking times in hours and estimated  $a$  and  $b$  with a unit of  $\log(\text{hour}^{-1})$ . However, the transformation between  $\log(\text{minute}^{-1})$  and  $\log(\text{hour}^{-1})$  is not clear, which makes their results incomparable. This problem is caused by the scale of the measurements. We call this problem

the problem of scale.

To solve the problem of scale, we propose a general method to revise the damage accumulation models by adding reference levels to the models. We define all parameters in the revised damage accumulation models to be unitless, and we scale the breaking times to be unitless before estimating the model parameters. In this approach, the estimates will be the same regardless of the unit of the measurements used in the experiments.

First, we consider the U.S. model:

$$\frac{d\alpha(t)}{dt} = \exp\{-a + b\sigma(t)\}.$$

We notice that  $\sigma(t)$  is unitless by definition. If we define both  $a$  and  $b$  to be unitless, we need to add a unit quantity to the right side of the differential equation since the left side of the differential equation has a unit, which is the inverse of the unit of time. Based on this idea, we revise the U.S. model as:

$$\frac{d\alpha(t)}{dt} = \lambda \exp\{-a + b\sigma(t)\}, \quad (27)$$

where  $\lambda = 1 \text{ hour}^{-1}$ , and  $a$  and  $b$  are unitless model parameters. By introducing the unit quantity  $\lambda$ , the solutions for  $T_s$  and  $T_c$  in the revised U.S. model are changed. Here, we show the solutions for  $T_s$  and  $T_c$  in the revised Foschi and Yao's version of the U.S. model. The idea can be applied to Gerhards and Link's version of the U.S. model without difficulty.

We can also choose  $\lambda = 1 \text{ minute}^{-1}$ , or the inverse of other units of measurement of time. The magnitude of the estimates will change accordingly.

For the ramp load test, the breaking time  $T_s$  is now given by

$$\lambda T_s = \frac{\exp(a)b}{\exp(b) - 1}. \quad (28)$$

For the constant load test, the breaking time  $T_c$  is now given by

$$\lambda T_c = \begin{cases} Ab, & \text{if } Ab \leq \lambda T_0, \\ \lambda T_0 + A \{\exp(b - \lambda T_0/A) - 1\}, & \text{if } Ab > \lambda T_0, \end{cases} \quad (29)$$

where  $A = \exp(a)/\{\exp(b) - 1\}$ .

We notice that by adding the unit quantity  $\lambda$  to the model, we scale the breaking times  $T_s$  and  $T_c$  to be unitless. In the revised model, the parameter estimates will be consistent regardless of the unit of measurements of the breaking times since both  $a$  and  $b$  are unitless. Because  $\lambda$  is a unit quantity which is set as  $1 \text{ hour}^{-1}$  and does not need to be estimated, adding  $\lambda$  will not complicate the estimation of the parameters.

The Madison Curve model can be revised in the same way as the U.S. model.

Now we consider the Canadian model

$$\frac{d\alpha(t)}{dt} = a\{\tau(t) - \sigma_0\tau_s\}_+^b + c\{\tau(t) - \sigma_0\tau_s\}_+^n\alpha(t), \quad (30)$$

where the problem of scale also appears. First, as polynomial functions, the terms  $\{\tau(t) - \sigma_0\tau_s\}_+^b$  and  $\{\tau(t) - \sigma_0\tau_s\}_+^n$  in (30) need to be unitless for the sake of unit comparability. However, the stress  $\tau(t)$  and the short term strength  $\tau_s$  have the unit of pressure while the threshold stress ratio  $\sigma_0$  does not have a unit by definition. So the terms  $\{\tau(t) - \sigma_0\tau_s\}_+^b$  and  $\{\tau(t) - \sigma_0\tau_s\}_+^n$  are not unitless in the Canadian model (30). One possible revision is to replace  $\{\tau(t) - \sigma_0\tau_s\}_+^b$  and  $\{\tau(t) - \sigma_0\tau_s\}_+^n$  in (30) by the unitless terms  $\{\sigma(t) - \sigma_0\}_+^b$  and  $\{\sigma(t) - \sigma_0\}_+^n$  respectively.

Second, the two sides of the differential equation (30) should have the same units if the model parameters  $a, b, c, n$  and  $\sigma_0$  are considered as unitless. By introducing two unit quantities  $\lambda_1$  and  $\lambda_2$ , we revise the Canadian model as

$$\frac{d\alpha(t)}{dt} = \lambda_1 a\{\sigma(t) - \sigma_0\}_+^b + \lambda_2 c\{\sigma(t) - \sigma_0\}_+^n\alpha(t), \quad (31)$$

where  $\lambda_1 = \lambda_2 = 1 \text{ hour}^{-1}$  and  $a, b, c, n$  and  $\sigma_0$  are unitless parameters.

For the ramp load test, the breaking time  $T_s$  is now approximated by

$$\lambda_1 T_s \approx \frac{b+1}{a(1-\sigma_0)^{b+1}}. \quad (32)$$

For the constant load test, the breaking time  $T_c$  is now approximated by

$$T_c \approx \begin{cases} \lambda_1^{-1} \frac{b+1}{a(1-\sigma_0)^{b+1}}, & \text{if } \frac{b+1}{a(1-\sigma_0)^{b+1}} \leq \lambda_1 T_0, \\ T_0 + \lambda_2^{-1} \frac{1}{c(\sigma_a - \sigma_0)^n} \ln \left\{ \frac{1 + (a/c)(\sigma_a - \sigma_0)^{b-n}}{\alpha_0 + (a/c)(\sigma_a - \sigma_0)^{b-n}} \right\}, \\ \text{if } \frac{b+1}{a(1-\sigma_0)^{b+1}} > \lambda_1 T_0, \end{cases} \quad (33)$$

where  $\alpha_0 \approx \{(1 - \sigma_0)/(\sigma_a - \sigma_0)\}^{b+1}$ .

In conclusion, the damage accumulation models can be revised by adding one or more unit quantities to solve the problem of scale. After revising the models, all parameters to be estimated are unitless, and the breaking times are scaled before the estimation procedures, so the estimation results will not depend on the units of the measurements used in the experiments.

## 4 Some results based on simulated data

In this section, we perform simulation studies to generate the breaking times in the ramp load test and in the constant load test based on the U.S. model and the Canadian model. The main objectives of this simulation study are (1) to investigate the effects of the assumed distributions of the random effects on the breaking times in the U.S. model, (2) to compare the data simulated from both the Canadian and U.S. models to the data collected by Foschi and Yao (1986) and (3) to fit the Weibull distribution, the log-normal distribution, the Normal distribution, and the exponential distribution to the data generated from both models.

For the simulations based on the U.S. model, we treat the model parameters  $a$  and  $b$  as random effects. We adopt our revision of Foschi and Yao's (1986) version of the U.S. model to get the solution for the breaking time  $T_s$  in the ramp load test and the solution for the breaking time  $T_c$  in the constant load test, as discussed in Section 3.4. We generate random effects that are Normal and/or log-normal, and study the effects of the mean, standard deviation, and the type of distribution on the distribution of the breaking times.

For the simulation based on the Canadian model, we adopt Foschi and Yao's approach to get the approximate solution for the breaking time  $T_s$  in the ramp load test and the solution for the breaking time  $T_c$  in the constant load test, as discussed in Section 3.3.

Here, all comparisons are made on the logarithm of the breaking times.

#### 4.1 Generating data based on the U.S. model

In this section, we generate the breaking time  $T_s$  in the ramp load test and breaking time  $T_c$  in the constant load test based on our revision of Foschi and Yao's version of the U.S. model, as shown in (27), and compare the distributions of the generated breaking times based on different assumptions for the random effects,  $a$  and  $b$ . We consider different distributions for  $a$  and  $b$ , including different means and standard deviations. Based on the revised Foschi and Yao's version of the U.S. model, we actually generate the scaled breaking times  $\lambda T_s$  and  $\lambda T_c$  in this study rather than  $T_s$  and  $T_c$ . However, for simplicity, we still refer to the generated values as  $T_s$  and  $T_c$ .

##### Summary of the U.S. model

Recall that our revision of Foschi and Yao's version of the U.S. model is given by

$$\frac{d\alpha(t)}{dt} = \lambda \exp\{-a + b\sigma(t)\}. \quad (34)$$

where  $\lambda = 1 \text{ hour}^{-1}$ ,  $a$  and  $b$  are unitless model parameters, and  $\tau_s$  is the short term strength, which is defined as the breaking strength of the wood specimen in the ramp load test when the ramp loading rate  $k$  is set so that the mean breaking time is around one minute.

The breaking time  $T_s$  in the ramp load test is given by:

$$\lambda T_s = \frac{\exp(a)b}{\exp(b) - 1}. \quad (35)$$

The breaking time  $T_c$  in the constant load test is given by:

$$\lambda T_c = \begin{cases} \frac{\exp(a)b}{\exp(b) - 1}, & \text{if } \frac{\exp(a)b}{\exp(b) - 1} \leq \lambda T_0, \\ \lambda T_0 + \frac{\exp(a)}{\exp(b) - 1} \left[ \exp \left\{ b - \lambda T_0 \frac{\exp(b) - 1}{\exp(a)} \right\} - 1 \right], & \\ \text{if } \frac{\exp(a)b}{\exp(b) - 1} > \lambda T_0 \end{cases}, \quad (36)$$

where  $T_0$  is the loading time in the ramp loading part of the constant load test.

To generate  $T_s$ , we need to specify the distributions of  $a$  and  $b$ , while to generate  $T_c$ , we need to specify the loading time  $T_0$  in the loading part of the constant load test, along with the distributions of  $a$  and  $b$ .  $T_0$  is usually set to be the  $p$ -th percentile of the generated  $T_s$  in the ramp load test.

We notice that, in the solution (35) for  $T_s$ , we do not need to specify the loading rate  $k$ , which implies that the distribution of random effects  $a$  and  $b$  should depend on the loading rate  $k$ . Otherwise, equation (35) would imply that the breaking times do not depend on the loading rate  $k$ , which contradicts the fact that, in experiments, the breaking times are shorter if the loading rate is large.

We also notice that the constant load  $\tau_a$  does not appear explicitly in the solution (36) for  $T_c$  in the U.S. model. However,  $\tau_a$  is actually included in the solution (36) since  $T_0 = \tau_a/k$ .

### Simulation setups

We denote the means of  $a$  and  $b$  by  $\mu_a$  and  $\mu_b$  respectively and denote the standard deviations of  $a$  and  $b$  by  $\sigma_a$  and  $\sigma_b$  respectively. In all simulation studies, we assume that  $a$  and  $b$  are independent.

To generate  $T_s$ , we generate  $n_s = 1000$   $a$ 's and  $b$ 's from the assumed distributions with means  $\mu_a$  and  $\mu_b$  respectively and standard deviations  $\sigma_a$  and  $\sigma_b$  respectively, and then calculate  $T_s$  from (35) based on the pairs of  $a$  and  $b$ .

To generate  $T_c$ , we choose  $T_0$  as the  $p$ -th percentile of the generated  $T_s$ 's, and then generate  $T_c$ 's based on another  $n_c = 1000$   $a$ 's and  $b$ 's, which are independent of the  $a$ 's and  $b$ 's we generated for  $T_s$ .

### The effect of distribution-type of $a$ and $b$ on the breaking times

In this section, we will investigate the effects of the choice of the distribution of the random effects on the generated breaking times  $T_s$  and  $T_c$ . So far, to our knowledge, random effects have not previously been used in the U.S. model. However, researchers have used random effects in other damage accumulation models, assuming that the random effects follow log-normal distributions, as in Foschi and Yao (1986).

In this study, we compare three different types of distributional assumptions on the random effects  $a$  and  $b$ : (1)  $a$  and  $b$  are both Normal, (2)  $a$  and  $b$  are both log-normal, and (3)  $a$  is Normal and  $b$  is log-normal. We compare the differences of the generated breaking times from the three scenarios when the means and the standard deviations of  $a$  and  $b$  are the same.

For the means  $\mu_a$  and  $\mu_b$  of the random effects  $a$  and  $b$ , we use  $\mu_a = 42$  and  $\mu_b = 50$ . We choose these values based on our estimates from the real data from Foschi and Yao's experiments. These values are similar to those in the literature: Gerhards and Link (1986) considered  $a$  and  $b$  as fixed across all wood specimens and estimated them as  $\hat{a} = 43.17$  and  $\hat{b} = 49.75$ .

Table 2 summarizes the setups of the simulation runs for studying the effect of the type of distribution of the random effects  $a$  and  $b$ . Results are displayed in Figure 5 to Figure 12.

Figure 5 to Figure 12 are generated when  $(\mu_a, \mu_b) = (42, 50)$  and  $p = 0.2$  for the constant load test. We use these figures to compare the distributions of  $T_s$  and  $T_c$  under the three different types of distribution of the random effects.

Figure 5 and Figure 6 show that the distributions of the generated  $\log_{10}(T_s)$  and  $\log_{10}(T_c)$  are similar under the three different distributional assumptions when the standard deviations  $\sigma_a$  and  $\sigma_b$  are both relatively small. This can be explained by the fact that when  $\sigma_a$  and  $\sigma_b$  are both relatively small, the Normal distribution and the log-normal distribution are similar and, as a result, the distributions of the generated breaking times  $T_s$  and  $T_c$  are similar.

Figure 7 shows results similar to those in Figure 5. The distributions of the generated  $\log_{10}(T_s)$  are roughly the same under the three different distributional assumptions, although there are observable differences in the

Breaking times	$a$		$b$		Figure for $T_s$ ( $T_c$ )
	Distribution	$\sigma_a$	Distribution	$\sigma_b$	
$T_s(T_c)$	Normal	1	Normal	1	Figure 5 (6)
$T_s(T_c)$	Normal	1	log-normal	1	Figure 5 (6)
$T_s(T_c)$	log-normal	1	log-normal	1	Figure 5 (6)
$T_s(T_c)$	Normal	10	Normal	10	Figure 7 (8)
$T_s(T_c)$	Normal	10	log-normal	10	Figure 7 (8)
$T_s(T_c)$	log-normal	10	log-normal	10	Figure 7 (8)
$T_s(T_c)$	Normal	10	Normal	1	Figure 9 (10)
$T_s(T_c)$	Normal	10	log-normal	1	Figure 9 (10)
$T_s(T_c)$	log-normal	10	log-normal	1	Figure 9 (10)
$T_s(T_c)$	Normal	1	Normal	10	Figure 11 (12)
$T_s(T_c)$	Normal	1	log-normal	10	Figure 11 (12)
$T_s(T_c)$	log-normal	1	log-normal	10	Figure 11 (12)

Table 2: Summary of the setups of the simulation runs for studying the effect of the type of distribution of the random effects  $a$  and  $b$  when  $\mu_a = 42$  and  $\mu_b = 50$ , and  $p = 0.2$  for the constant load test.

lower tail and the upper tail of the distribution of the generated  $\log_{10}(T_s)$ . The differences can be explained by the fact that the log-normal distribution is heavy-tailed, so the distribution of the generated  $\log_{10}(T_s)$  is heavy-tailed when  $\sigma_a$  and  $\sigma_b$  are large.

Figure 8 shows that the distributions of the generated  $\log_{10}(T_c)$  are different under the three distributional assumptions, especially in the centre of the distribution. In other words, those generated breaking times  $T_c$  which are slightly larger than the loading time  $T_0$  are more sensitive to the distributional assumptions of the random effects  $a$  and  $b$  when  $\sigma_a$  and  $\sigma_b$  are large.

Figure 9 and Figure 10 show that the distributions of the generated  $\log_{10}(T_s)$  and  $\log_{10}(T_c)$  are mainly affected by the distributional assumptions on  $a$  when  $\sigma_a$  is relatively large and  $\sigma_b$  is relatively small. The lower left panels of Figure 9 and Figure 10 show that the distribution of the generated  $\log_{10}(T_s)$  and the distribution of the generated  $\log_{10}(T_c)$  both stay roughly the same when the distributional assumption on  $b$  changes from Normal to log-normal. However, from the lower right panels of Figure 9 and Figure 10,

the distributions of the breaking times are quite different when the distributional assumption on  $a$  changes from Normal to log-normal, which means the distributional assumption on  $a$  has an effect on the distribution of  $\log_{10}(T_s)$  and  $\log_{10}(T_c)$ .

Figure 11 and Figure 12 show that the distributions of the generated  $\log_{10}(T_s)$  and  $\log_{10}(T_c)$  are mainly affected by the distributional assumption on  $b$  when  $\sigma_a$  is relatively small and  $\sigma_b$  is relatively large. The lower right panels of Figure 11 and Figure 12 show that the distribution of the generated  $\log_{10}(T_s)$  and the distribution of the generated  $\log_{10}(T_c)$  both stay roughly the same when the distributional assumption on  $a$  changes from Normal to log-normal. However, from the lower left panels of Figure 11 and Figure 12, the distributions of the generated breaking times are different when the distributional assumption on  $b$  changes from Normal to log-normal, which means the distributional assumption on  $b$  has an effect on the distribution of  $\log_{10}(T_s)$  and  $\log_{10}(T_c)$ .

In conclusion, the distributions of  $T_s$  and  $T_c$  are not greatly affected by the distributional assumptions if the standard deviations of both random effects  $a$  and  $b$  are relatively small. The distributions of  $T_s$  and  $T_c$  are mainly affected by the distributional assumption on the random effect with a large standard deviation, and not greatly affected by the distributional assumption on the random effect with a small standard deviation.

### **The effect of the means and standard deviations of $a$ and $b$ on the breaking times**

In this section, we assume that both  $a$  and  $b$  are Normal, and investigate the effects of the means and the standard deviations of  $a$  and  $b$  on the breaking times  $T_s$  and  $T_c$ .

We investigate the effects of the means of the random effects  $a$  and  $b$  on the breaking times  $T_s$  and  $T_c$  by fixing the standard deviations of  $a$  and  $b$ . First, we compare the empirical cumulative distributions of the generated  $T_s$ 's and  $T_c$ 's as a function of  $\mu_a$  with  $\sigma_a, \sigma_b$  and  $\mu_b$  fixed. Second, we compare the empirical cumulative distributions of the generated  $T_s$ 's and  $T_c$ 's as a function of  $\mu_b$  with  $\sigma_a, \sigma_b$  and  $\mu_a$  fixed.

Similarly, we investigate the effects of the standard deviations of the random effects of  $a$  and  $b$  on the breaking times  $T_s$  and  $T_c$  by fixing the means of  $a$  and  $b$ .

Table 3 summarizes the setups of the simulation runs for studying the

effect of the mean and the standard deviation of the random effects  $a$  and  $b$  when  $a$  and  $b$  are both Normal. Results are displayed in Figure 13 and Figure 14.

Figure 13 compares the empirical cumulative distributions of the generated  $\log_{10}(T_s)$  and the empirical cumulative distributions of the generated  $\log_{10}(T_c)$  based on the assumption that  $a$  and  $b$  are both Normal,  $\sigma_a = 1$  and  $\sigma_b = 1$  are fixed, and either  $\mu_a$  or  $\mu_b$  is not fixed. Figure 14 shows the comparisons of the empirical cumulative distributions of the generated  $\log_{10}(T_s)$  and the empirical cumulative distributions of the generated  $\log_{10}(T_c)$  based on the assumption that  $a$  and  $b$  are both Normal,  $\mu_a = 42$  and  $\mu_b = 50$  are fixed, and either  $\sigma_a$  or  $\sigma_b$  is not fixed.

$T$	$a$		$b$		Figure
	$\mu_a$	$\sigma_a$	$\mu_b$	$\sigma_b$	
$T_s$ and $T_c$	37	1	50	1	Figure 13
$T_s$ and $T_c$	42	1	50	1	Figure 13
$T_s$ and $T_c$	47	1	50	1	Figure 13
$T_s$ and $T_c$	42	1	45	1	Figure 13
$T_s$ and $T_c$	42	1	50	1	Figure 13
$T_s$ and $T_c$	42	1	55	1	Figure 13
$T_s$ and $T_c$	42	1	50	1	Figure 14
$T_s$ and $T_c$	42	3	50	1	Figure 14
$T_s$ and $T_c$	42	5	50	1	Figure 14
$T_s$ and $T_c$	42	1	50	1	Figure 14
$T_s$ and $T_c$	42	1	50	3	Figure 14
$T_s$ and $T_c$	42	1	50	5	Figure 14

Table 3: Summary of the setups of the simulation runs for studying the effect of the mean and the standard deviation of the random effects  $a$  and  $b$  when  $a$  and  $b$  are both Normal, and  $p = 0.2$  in the constant load test.

Figure 13 shows that the means of the random effects  $a$  and  $b$  mainly affect the locations of the distributions of the breaking times. In the upper left panel, upper right panel and the lower left panel, the location shifts are uniform over the range of the generated breaking times. In the lower right panel, the location shift effect is significant in the lower part of the distribution of the generated  $T_c$ , but is small in the upper part of the distribution

of the generated  $T_c$ . This panel shows that the magnitude of  $\mu_b$  affects the breaking time more for small values of  $T_c$ , and does not affect the maximum breaking time  $T_c$  in the constant load test. The two upper panels also show that the generated  $T_s$ 's and  $T_c$ 's increase when  $\mu_a$  increases, and the two lower panels show that the generated  $T_s$ 's and  $T_c$ 's decrease when  $\mu_b$  increases since  $\log(T_s) = a + \log(b) - \log\{\exp(b) - 1\}$ , the effect of  $\mu_a$  on  $T_s$ 's distribution is clear. Since  $\exp(b)$  dominates  $b$ , the effect of  $\mu_b$  is also clear. For  $T_c$ , this cannot be explained easily since the solution (36) is complicated. From Figure 13, we also notice that in order to generate reasonable breaking times  $T_s$ , i.e., with the mean of  $T_s$ 's around 1 minute,  $\mu_a - \mu_b$  should be between 5 and 10.

Figure 14 shows that the standard deviations of the random effects  $a$  and  $b$  mainly affect the shapes of the distributions of the breaking times. The variation among the generated  $T_s$ 's and the variation among the generated  $T_c$ 's increase when either  $\sigma_a$  or  $\sigma_b$  increases. The breaking times  $T_c$ 's in the constant load test concentrate more in the upper tail when either  $\sigma_a$  or  $\sigma_b$  is large. In other words, if  $\sigma_a$  and  $\sigma_b$  are small, we would expect more boards to break during the early stage of the constant load test, and if either  $\sigma_a$  or  $\sigma_b$  is large, we would expect few boards to break during the early stage of the constant load test and more boards to break at almost the same time at the late stage in the constant load test.

In conclusion, the locations of the distributions of the generated  $T_s$  and  $T_c$  are mainly affected by the means of the random effects  $a$  and  $b$ , and the shapes of the distributions of the generated  $T_s$  and  $T_c$  are mainly affected by the standard deviations of the random effects  $a$  and  $b$ .

## 4.2 Generating data based on the Canadian model

In this section, we generate the breaking time  $T_c$  in the constant load test based on the Canadian model using the parameter estimates from Foschi and Yao (1986).

In Section 3.3 and Section 3.4, we discussed the Canadian model and the revised Canadian model. The forms of the solutions for the breaking times of the Canadian model and those of the revised Canadian model are different, unlike the solutions for the breaking times of the U.S. model and those of the revised U.S. model, which only differ by a unit quantity  $\lambda$ . To use the parameter estimates from Foschi and Yao (1986), we adopt the Canadian model in this section for generating breaking times because Foschi and Yao

estimated the parameters using the Canadian model.

### Summary of the Canadian model

Recall that the Canadian model is given by

$$\frac{d\alpha(t)}{dt} = a\{\tau(t) - \sigma_0\tau_s\}_+^b + c\{\tau(t) - \sigma_0\tau_s\}_+^n\alpha(t), \quad (37)$$

where  $a, b, c, n$  and  $\sigma_0$  are model parameters.

For the ramp load test, the breaking time  $T_s$  is approximated by

$$T_s \approx \frac{\{k(b+1)/a\}^{1/(b+1)}}{k(1-\sigma_0)}. \quad (38)$$

For the constant load test, the breaking time  $T_c$  is approximated by

$$T_c \approx \begin{cases} \frac{\{k(b+1)/a\}^{1/(b+1)}}{k(1-\sigma_0)}, & \text{if } \frac{\{k(b+1)/a\}^{1/(b+1)}}{k(1-\sigma_0)} \leq T_0, \\ T_0 + \frac{1}{c(\tau_a - \sigma_0\tau_s)^n} \ln \left\{ \frac{1 + (a/c)(\tau_a - \sigma_0\tau_s)^{b-n}}{\alpha_0 + (a/c)(\tau_a - \sigma_0\tau_s)^{b-n}} \right\}, \\ \text{if } \frac{\{k(b+1)/a\}^{1/(b+1)}}{k(1-\sigma_0)} > T_0, \end{cases} \quad (39)$$

with  $a$  approximated by

$$a \approx \frac{k(b+1)}{\{\tau_s(1-\sigma_0)\}^{b+1}}, \quad (40)$$

and  $\alpha_0$  approximated by

$$\alpha_0 \approx \left( \frac{\tau_a - \sigma_0\tau_s}{\tau_s - \sigma_0\tau_s} \right)^{b+1}. \quad (41)$$

We discussed Foschi and Yao's method of parameter estimation in Section 3.3. They treated  $b, c, n$  and  $\sigma_0$  as independent random effects which follow log-normal distributions with means  $\mu_b, \mu_c, \mu_n$  and  $\mu_{\sigma_0}$  and standard deviations  $\sigma_b, \sigma_c, \sigma_n$  and  $\sigma_{\sigma_0}$  respectively. They treated  $\tau_s$  as a random effect,

which is independent of  $b, c, n$  and  $\sigma_0$ , with distribution equal to the empirical distribution of the short term strength of the wood specimens in the one minute ramp load test. They treated  $a$  as another random effect, but did not need to specify its distribution since  $a$  can be expressed in terms of the other random effects.

They obtained the following estimates: the means of  $b, c, n$  and  $\sigma_0$  are estimated by 35.204,  $0.1559 \times 10^{-6}$ , 1.429 and 0.578 respectively and the standard deviations of  $b, c, n$  and  $\sigma_0$  are estimated by 6.589,  $0.9621 \times 10^{-7}$ , 0.139 and 0.163 respectively. We should be aware that these are estimates of the means and variances of the log-normal distributed random effects, but not the parameters we usually use to characterize log-normal distributions.

### Simulation setups

In this section, we describe the setups of generating simulated breaking times based on the Canadian model.

As discussed in the previous section, we have the estimates of the distributions of the random effects  $b, c, n$  and  $\sigma_0$  from Foschi and Yao (1986). We also have the loading rate  $k = 6474 \times 60$  psi/hour from Foschi and Barrett (1982). We need the distribution of either  $\tau_s$  or  $a$  to generate the breaking time  $T_c$  in the constant load test. These distributions are not available to us.

There are two alternatives for generating the breaking time  $T_c$ . We can generate  $\tau_s$  using the U.S. model and then calculate  $a$  from (40) given  $\tau_s$ , or we can generate  $a$  based on some distribution and then calculate  $\tau_s$  from (40) given  $a$ . We adopt the first approach in this section since we do not have much information on the distribution of  $a$ .

The procedures for generating  $T_c$  based on the Canadian model are described as follows. First, we generate  $n_s = 1000$   $T_s$ 's from the U.S. model when  $(\mu_a, \mu_b, \sigma_a, \sigma_b) = (42, 50, 0.4, 0.4)$  and we calculate  $\tau_s$  using the fact that  $T_s = \tau_s/k$  in Foschi and Yao's version of the U.S. model. Second, we generate  $n_c = 1000$   $b$ 's,  $c$ 's,  $n$ 's and  $\sigma_0$ 's from the log-normal distributions with the means  $\mu_b = 35.204$ ,  $\mu_c = 0.1559 \times 10^{-6}$ ,  $\mu_n = 1.429$  and  $\mu_{\sigma_0} = 0.578$  respectively and the standard deviations  $\sigma_b = 6.589$ ,  $\sigma_c = 0.9621 \times 10^{-7}$ ,  $\sigma_n = 0.139$  and  $\sigma_{\sigma_0} = 0.163$  respectively. Third, we calculate  $a$  from (40) and  $\alpha_0$  from (41) for the vector  $(\tau_s, b, c, n, \sigma_0)$ , and then calculate the breaking time  $T_c$  from (39).

In the following sections, we compare the generated breaking times to those in Foschi and Yao's data (Section 4.3) and we fit standard models to

the breaking times (Section 4.4).

### 4.3 Comparisons of the generated data with Foschi and Yao's data

In this section, we compare the generated breaking times based on the U.S. model and the Canadian model from the previous sections with the breaking times from Foschi and Yao's experiments. We do not discuss parameter estimation in this section.

The empirical distribution of the logarithm of the breaking times  $T_c$ 's from Foschi and Yao's experiments are shown in Figure 15. According to Foschi and Yao (1986), the constant load was set to be the 20-th percentile of the short term strength in their ramp load test. We do not have the data from their ramp load test.

By trial and error, we find that the empirical distribution of the generated breaking time  $T_c$  is close to the empirical distribution of the breaking time  $T_c$  from Foschi and Yao's experiments when  $(\mu_a, \mu_b, \sigma_a, \sigma_b) = (42, 50, 0.4, 0.4)$  in the U.S. model, as shown in the left panel of Figure 15. The empirical distribution of the generated breaking time  $T_c$  based on the Canadian model is shown in the right panel of Figure 15 for comparison.

The left panel of Figure 15 shows that the empirical distribution of the generated breaking time  $T_c$  based on the U.S. model and the empirical distribution of the breaking time  $T_c$  from Foschi and Yao's experiments do not seem consistent overall. However, the two curves are in close agreement over the ramp loading part, i.e., when  $T_c \leq T_0$ , but differ in the constant load part, i.e., when  $T_c > T_0$ . In particular, in the dataset, the percentage of wood specimens breaking increases rapidly for the times with  $\log_{10}(T_c) > 2$ .

The right panel of Figure 15 also shows that the empirical distribution of the generated breaking times  $T_c$ 's based on the Canadian model differs from the empirical distribution of the breaking times  $T_c$ 's from Foschi-Yao experiments. Again, the two curves are close during the ramp loading part, but different during the constant load part. The percentage of the generated specimens that break shows the same rapid increase as does the percentage of the breaking specimens from the Foschi-Yao experiments. However, the rapid increase occurs later in the generated specimens.

The generated  $T_c$ 's based on the revised U.S. model or the Canadian model do not fit the data from the Foschi-Yao experiments well. In an

attempt to improve the fit, we tried various values for  $\mu_a$ ,  $\mu_b$ ,  $\sigma_a$  and  $\sigma_b$  in the U.S. model and various values for  $k$  in the Canadian model. For the values we tried, the empirical distribution function of the breaking times  $T_c$ 's generated from the U.S. model did not show the rapid increase at the same stage as the data from the Foschi-Yao experiments. The empirical distribution function of the breaking times  $T_c$ 's generated from the Canadian model is closer to that of the data from the Foschi-Yao experiments when  $k$  is large.

#### 4.4 Fitting the generated failure strengths to distributions

In this section, we investigate the type of distribution of the generated breaking times based on the U.S. model and the Canadian model. We simulate breaking times from each model as described in Sections 4.1 and 4.2. We then fit the Weibull distribution, the log-normal distribution, the Normal distribution and the exponential distribution to the simulated data.

In this section, we study the breaking times  $T = T_s$  in the ramp load test, and  $T = T_c - T_0$  for  $T_c > T_0$  in the constant load test. We do not separately consider the distribution of  $T_c$  for  $T_c \leq T_0$  because by definition,  $P(T_c \leq t) = P(T_s \leq t)$  whenever  $t \leq T_0$ .

We assess the fits of the parametric distributions as follows. First, we calculate the maximum likelihood estimates of the parameters of the distribution to be fitted using parametric models and the R-function *survreg*. For the breaking times generated from the U.S. model, there is no censoring, but for the breaking times generated from the Canadian model, there is censoring since some boards do not break during the constant load test. To study how well the fitted distribution matches that of the generated breaking times, we simulate  $n = 1000$   $T_{fit}$ 's from the fitted distribution. Then we draw the quantile-quantile plot of the logarithm of the generated breaking times  $T$ 's from the damage accumulation models and the logarithm of the simulated  $T_{fit}$ 's from the fitted distribution. The quantile-quantile plots are shown in Figure 16 to Figure 20.

Table 4 summarizes the setups of the simulation runs that produce Figure 16 to Figure 20.

In all scenarios, the Normal distribution and the exponential distribution fit the generated breaking times poorly, so we only show one set of quantile-

$T$	Model	Fitted distribution	$\sigma_a$	$\sigma_b$	Figure
$T_s$	U.S.	Weibull, log-normal, Normal & exponential	0.4	0.4	Figure 16
$T_s$	U.S.	Weibull & log-normal	10	10	Figure 17
$T_c$	U.S.	Weibull & log-normal	0.4	0.4	Figure 18
$T_c$	U.S.	Weibull & log-normal	10	10	Figure 19
$T_c$	Canadian	Weibull & log-normal	0.4	0.4	Figure 20

Table 4: Summary of the setups of the simulation runs for studying the distribution of the generated breaking times when  $\mu_a = 42$  and  $\mu_b = 50$ , and  $p = 0.2$  in the constant load test.

quantile plots for the Normal distribution and the exponential distribution. See Figure 16. The fitting results for the Weibull distribution and the log-normal distribution are shown in all figures in this section.

Figure 16 shows that the log-normal distribution fits generated breaking times  $T_s$ 's very well although there are slight differences in the lower tail and the upper tail. The other types of distribution do not provide reasonable fits for the generated breaking times.

Figure 17 shows similar results as in Figure 16. The log-normal distribution fits the generated breaking times  $T_s$ 's very well when the standard deviations of the random effects  $a$  and  $b$  are large, but the Weibull distribution fits the generated breaking times  $T_s$ 's poorly.

Figure 18 shows that neither the Weibull distribution nor the log-normal distribution fits the generated breaking times  $(T_c - T_0)$ 's for those  $T_c > T_0$  well as a whole. The left panel of Figure 18 shows that the Weibull distribution is heavier than the distribution of  $(T_c - T_0)$  in the lower tail, but provides a reasonable fit for other  $(T_c - T_0)$ 's. The right panel of Figure 18 shows that the log-normal distribution fits the distribution of  $(T_c - T_0)$  well in the centre of the distribution, but is heavier than the distribution of  $(T_c - T_0)$  in the lower tail and the upper tail.

Figure 19, where the standard deviations of the random effects  $a$  and  $b$  are large, shows similar results as in Figure 18. The left panel of Figure 19 shows that the Weibull distribution fits the distribution of  $(T_c - T_0)$  reasonably well although there are still minor differences in the lower tail and the centre. The right panel of Figure 19 shows that the fitted log-normal distribution is lighter than the distribution of  $(T_c - T_0)$  in the lower tail and heavier in the

upper tail.

Figure 20 shows similar results as in Figure 18 and Figure 19 when the breaking times  $T_c$ 's are generated from the Canadian model. The Weibull distribution fits the data  $(T_c - T_0)$ 's well except for the lower tail.

In conclusion, if the breaking times  $T_s$ 's are generated from the U.S. model under the conditions described, the  $T_s$ 's seem to follow a log-normal distribution and if the breaking times  $T_c$ 's are generated from the U.S. model or the Canadian model under the conditions described, all  $(T_c - T_0)$ 's which satisfy  $T_c > T_0$  and  $T_c - T_0$  not close to 0 seem to follow a Weibull distribution.

## 5 Concluding remarks

We believe this paper's review of damage models is timely. New manufactured lumber products are under active development and both the models and principles underlying their development will be needed in setting design values. A wealth of information is available on creep rupture and duration of load effect of lumber, panel products and glulam, and laminated veneer lumber (LVL). Strand-based products, such as laminated strand lumber (LSL) and oriented strand lumber (OSL) may have different creep and creep-rupture behaviour than solid lumber or veneer-based products, and changes to the composition or manufacturing parameters can easily change a product that has similar duration of load and creep effects as solid lumber to one that does not.

However, while a significant amount of information is available for duration of load and creep effects of lumber, limited information is available on structural composite lumber. It was found out that while some structural composite lumber products, such as LVL, have consistently demonstrated engineering equivalence to the duration of load of solid sawn lumber, such equivalence is more difficult to demonstrate for other structural composite lumber products, such as LSL and OSL, and more tests are necessary to define their creep and creep-rupture behaviour.

The increasingly global nature of the lumber industry points to a need to rationalize methods and procedures and we believe this review may assist in that way as well. North America, Europe and Japan have different methods for evaluating load duration and creep, and consequently Canada/United States, Europe and Japan have different standards on this topic. China is interested in having a standard in this area and is using ASTM D 6815 as a

seed document, while ISO will likely develop a standard based on one of the existing standards. Canada, United States and Japan have been discussing the duration of load topic but additional comparison data are necessary to come up with a resolution. Statistical tools will come in handy for such comparison and may pave the road for a mutually recognized method for assessing creep and duration of load effects. Our companion reports (Zhai 2012; Zhai et al. 2012) describe such tools.

## References

- [1] American Society for Testing and Materials (ASTM). ASTM D 6815 09. Standard Specification for Evaluation of Duration of Load and Creep Effects of Wood and Wood-Based Products. ASTM International, 100 Barr Harbor Drive, PO Box C700, West Conshohocken, PA 19428-2959, United States.
- [2] Barrett, J. D. and Foschi, R. O. (1978). Duration of load and probability of failure in wood. Part I: modelling creep rupture. *Canadian Journal of Civil Engineering*, Vol. 5, No. 4: 505–514.
- [3] Barrett, J. D. and Foschi, R. O. (1978). Duration of load and probability of failure in wood. Part II: constant, ramp and cyclic loadings. *Canadian Journal of Civil Engineering*, Vol. 5, No. 4: 515–532.
- [4] Cai, Z., Rosowsky, D. V., Hunt, M. O. and Fridley, K. J. (2000). Comparison of actual vs. simulated failure distributions of flexural wood specimens subject to 5-day load sequences. *Forest Products Journal*, 50(1): 74–80.
- [5] Faherty, K.F. and Williamson, T.G. (1995). *Wood Engineering and Construction Handbook*. ISBN 0-07-019911-6 McGraw-Hill, Inc. USA.
- [6] Foschi, R. O. and Barrett, J. D. (1982). Load-duration effects in western hemlock lumber. *ASCE Journal of the Structural Division*, Vol. 108(7): 1494–1510.
- [7] Foschi, R. O. and Yao, F. Z. (1986). Another look at three duration of load models. *In Proceedings of IUFRO Wood Engineering Group Meeting*, Florence, Italy, paper: 19-9-1.

- [8] Gerhards, C. C. (1977). Effects of duration and rate of loading on strength of wood and wood-based materials. *Madison: USDA Forest Services Research Report*, FPL 283.
- [9] Gerhards, C. C. (1979). Time-related effects of loading on wood strength: a linear cumulative damage theory. *Wood Science*, 11(3): 139–144.
- [10] Gerhards, C. C. and Link, C. L. (1987). A cumulative damage model to predict load duration characteristics of lumber. *Wood and Fiber Science*, 19(2): 147–164.
- [11] Gerhards, C. C. (1988). Effect of grade on load duration of Douglas - fir lumber in bending. *Wood and Fiber Science*, 20(1): 146–161.
- [12] Hendrickson, E. M., Ellingwood, B. and Murphy, J. (1987). Limit state probabilities for wood structural members. *Journal of Structural Engineering*, Vol. 113, No. 1, 88–106
- [13] Karacabeyli, E. and Soltis, L.A. (1991). State of the art report on duration of load research for lumber in North America. Proceedings of the 1991 International Timber Engineering Conference. London, United Kingdom.
- [14] Markwardt, L.J. and Liska, J.A. (1948). Speed of Testing of Wood. Factors in its Control and its Effect on Strength. *Proc. ASTM*, 48:1139–115.
- [15] Wang, J. B. (2009). Duration-of-load and creep behavior of thick MPB strand based wood composite. Ph.D. thesis. Faculty of Forestry, the University of British Columbia.
- [16] Wood, L. W. (1951). Relation of strength of wood to duration of load. *Madison: USDA Forest Service Report*, No. 1916.
- [17] Yao, F. Z. (1987). Reliability of structures with load history-dependent strength of an application to wood members. Master thesis, Department of Civil Engineering, the University of British Columbia.
- [18] Zhai, Y. (2012) Duration of Load models. MSc Thesis, Department of Statistics, the University of British Columbia.

- [19] Zhai, Y, Heckman, N., Lum, C. Pirvu, C. Wu, L. and Zidek, J.V. (2012). Statistical methods for fitting duration of load effects for lumber products. TR #, Department of Statistics, University of British Columbia.

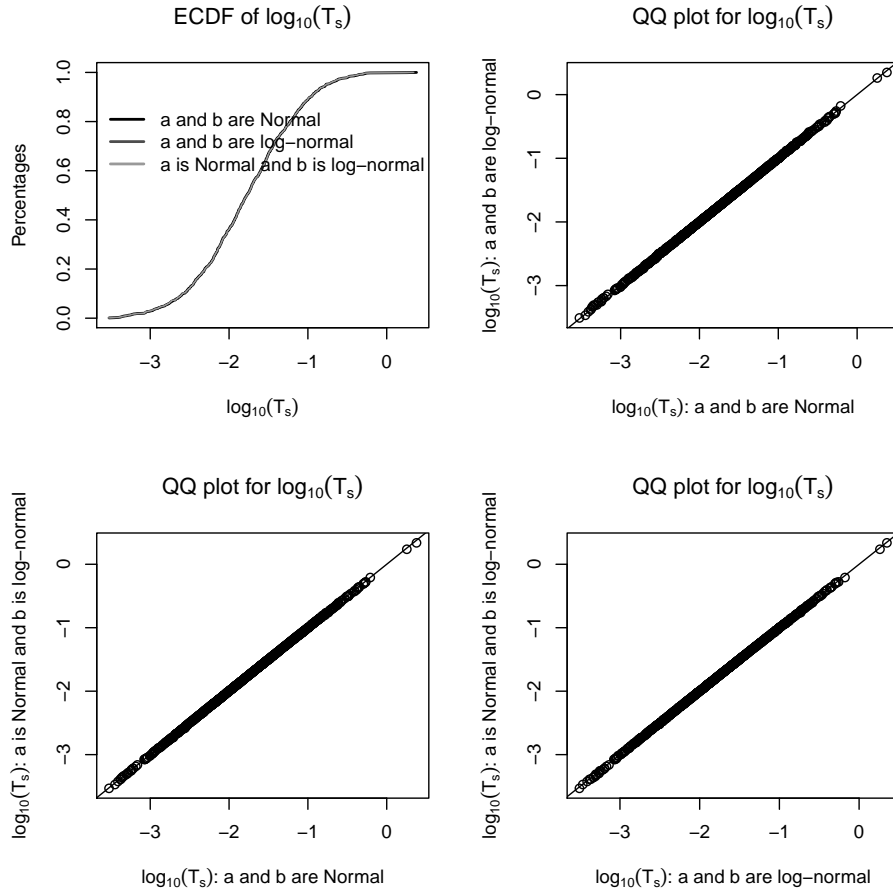


Figure 5: Comparisons of the generated  $T_s$  in the U.S. model based on the three different distributional assumptions of  $a$  and  $b$  when  $\mu_a = 42$ ,  $\mu_b = 50$ ,  $\sigma_a = 1$  and  $\sigma_b = 1$ . Upper left: the empirical cumulative distributions of  $\log_{10}(T_s)$  from the three scenarios. Upper right: the quantile-quantile plot of the generated  $\log_{10}(T_s)$  from the assumption that  $a$  and  $b$  are both Normal and the assumption that  $a$  and  $b$  are both log-normal. Lower left: the quantile-quantile plot of the generated  $\log_{10}(T_s)$  from the assumption that  $a$  and  $b$  are both Normal and the assumption that  $a$  is Normal and  $b$  is log-normal. Lower right: the quantile-quantile plot of the generated  $\log_{10}(T_s)$  from the assumption that  $a$  and  $b$  are both log-normal and the assumption that  $a$  is Normal and  $b$  is log-normal.

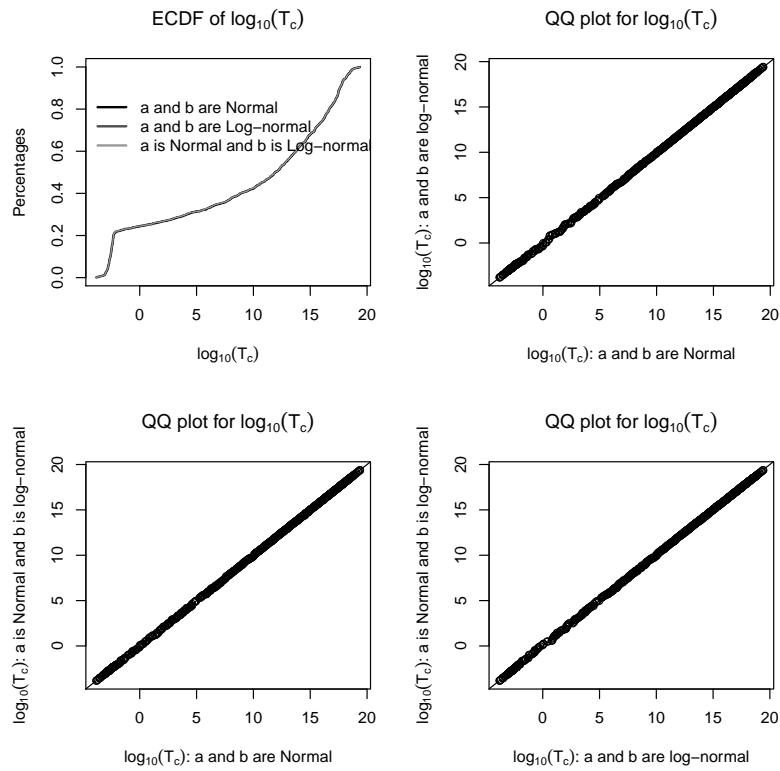


Figure 6: Comparisons of the generated  $T_c$  in the U.S. model based on the three different distributional assumptions of  $a$  and  $b$  when  $\mu_a = 42, \mu_b = 50, \sigma_a = 1, \sigma_b = 1$  and  $p = 0.2$ . The panels are in the same arrangement as in Figure 5.

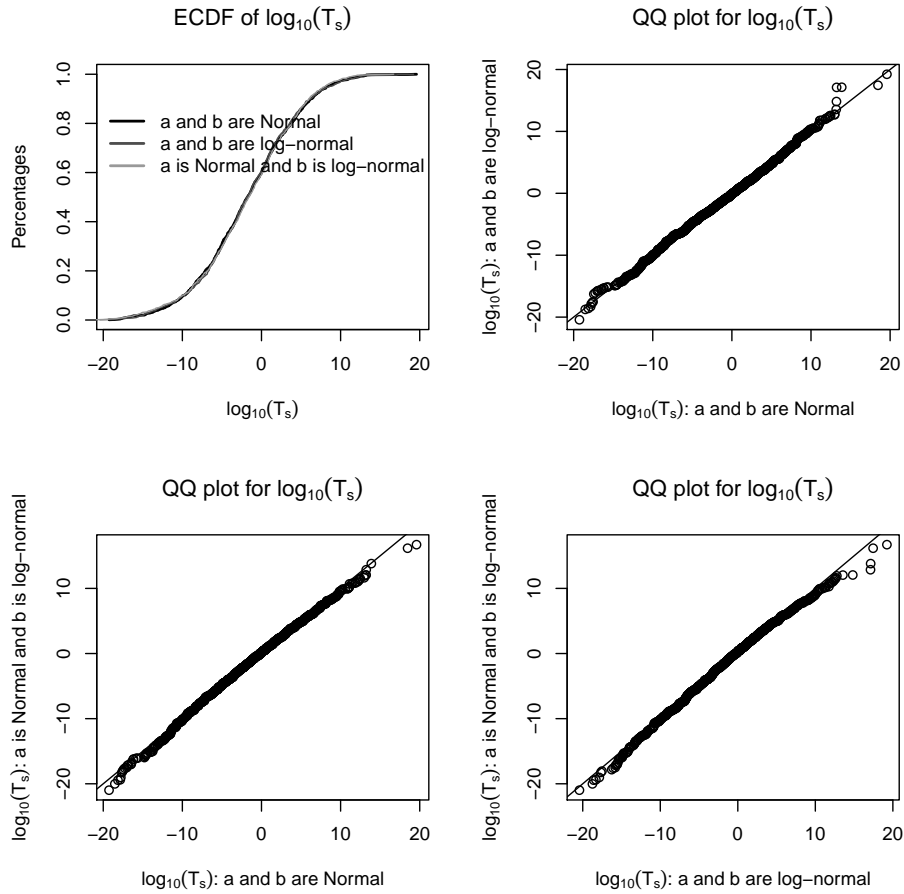


Figure 7: Comparisons of the generated  $T_s$  in the U.S. model based on the three different distributional assumptions of  $a$  and  $b$  when  $\mu_a = 42, \mu_b = 50, \sigma_a = 10$  and  $\sigma_b = 10$ . The panels are in the same arrangement as in Figure 5.

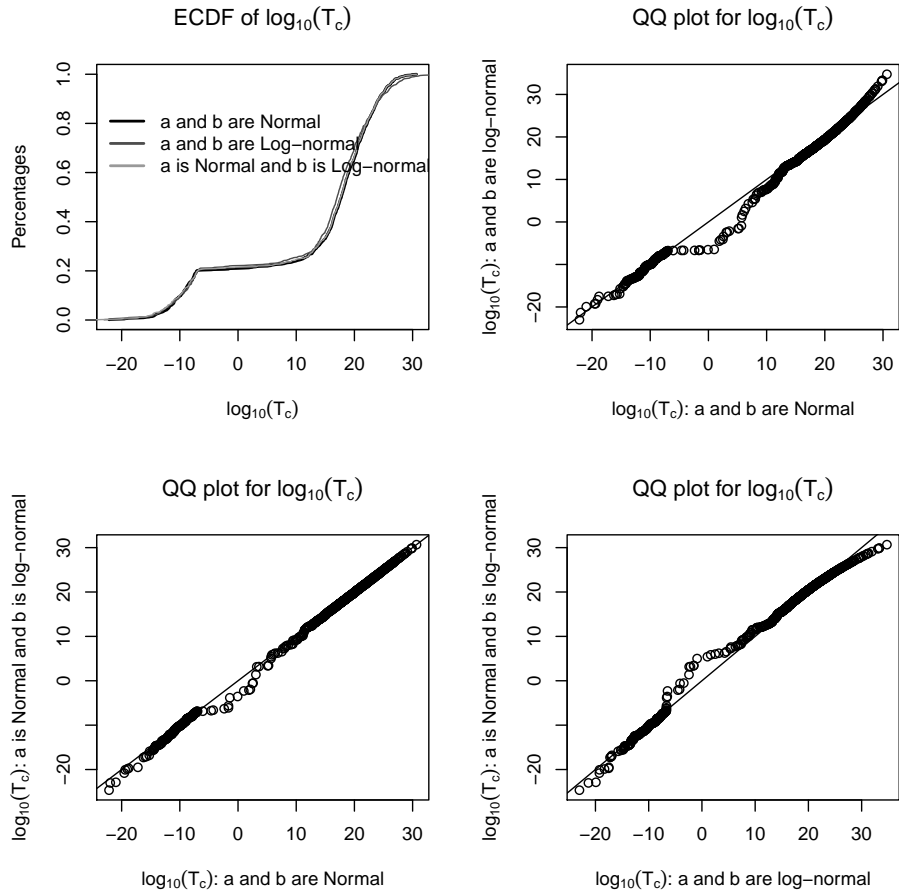


Figure 8: Comparisons of the generated  $T_c$  in the U.S. model based on the three different distributional assumptions of  $a$  and  $b$  when  $\mu_a = 42$ ,  $\mu_b = 50$ ,  $\sigma_a = 10$ ,  $\sigma_b = 10$  and  $p = 0.2$ . The panels are in the same arrangement as in Figure 5.

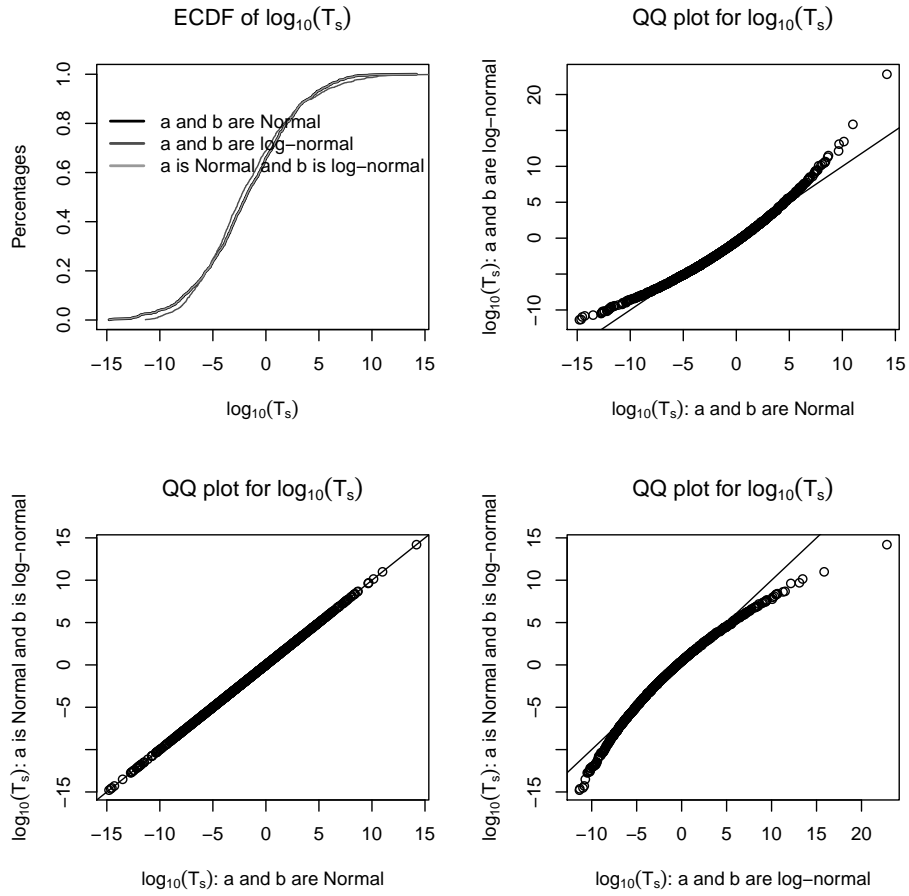


Figure 9: Comparisons of the generated  $T_s$  in the U.S. model based on the three different distributional assumptions of  $a$  and  $b$  when  $\mu_a = 42, \mu_b = 50, \sigma_a = 10$  and  $\sigma_b = 1$ . The panels are in the same arrangement as in Figure 5.

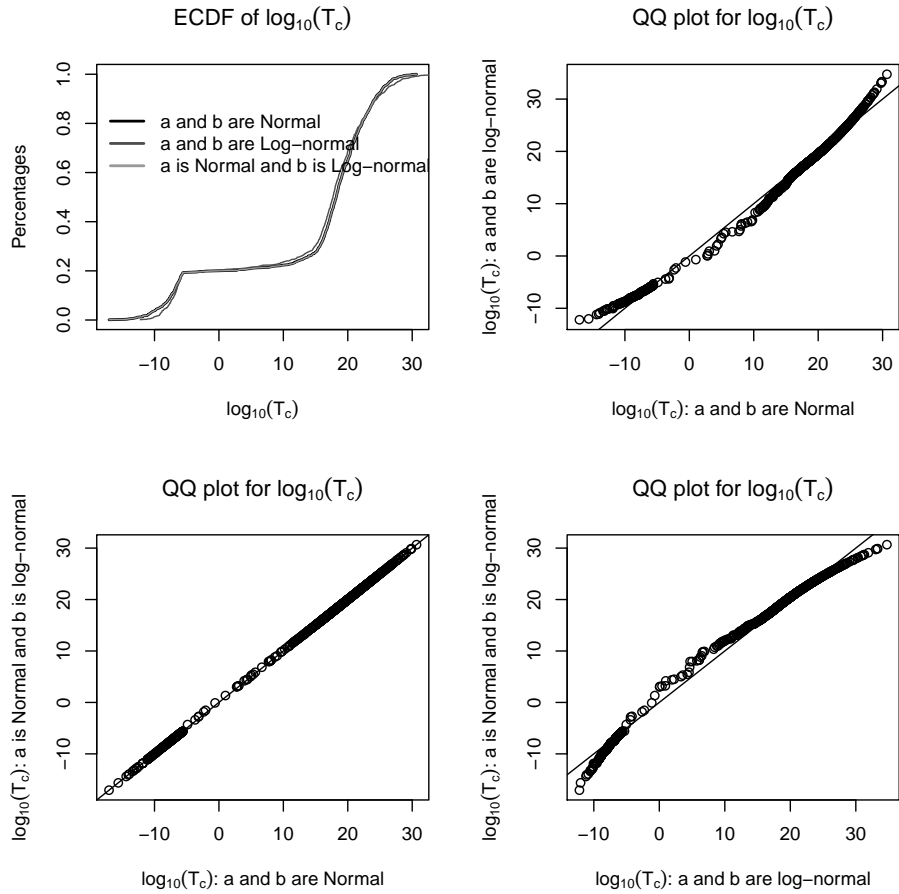


Figure 10: Comparisons of the generated  $T_c$  in the U.S. model based on the three different distributional assumptions of  $a$  and  $b$  when  $\mu_a = 42, \mu_b = 50, \sigma_a = 10, \sigma_b = 1$  and  $p = 0.2$ . The panels are in the same arrangement as in Figure 5.

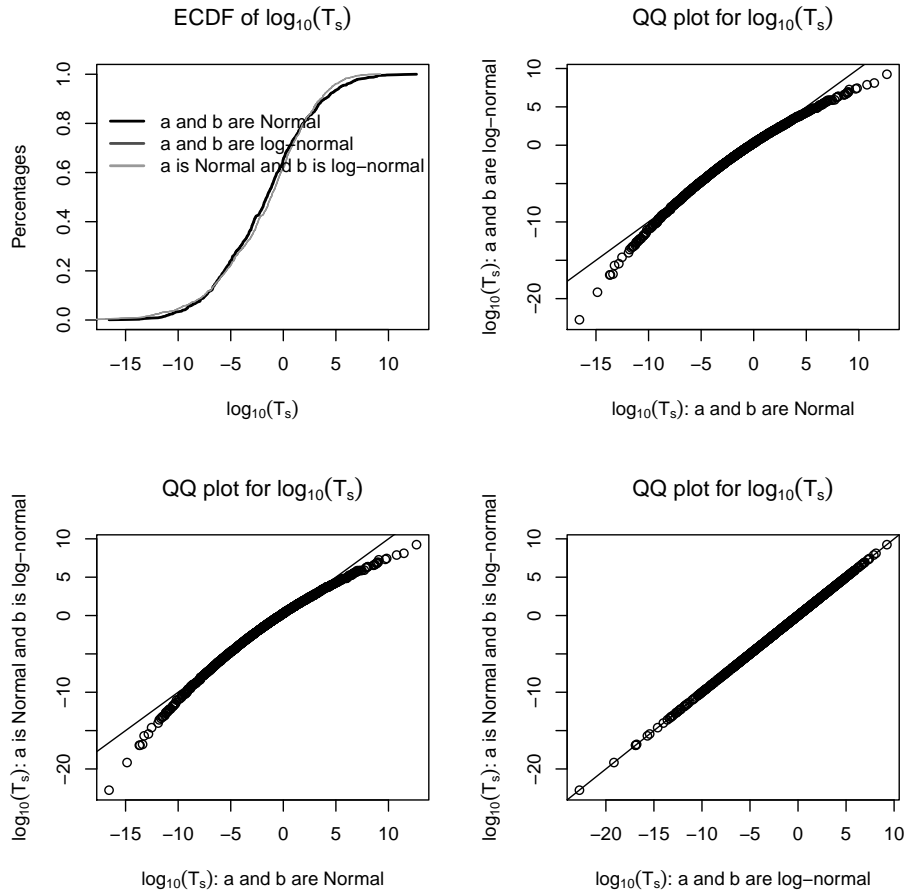


Figure 11: Comparisons of the generated  $T_s$  in the U.S. model based on the three different distributional assumptions of  $a$  and  $b$  when  $\mu_a = 42, \mu_b = 50, \sigma_a = 1$  and  $\sigma_b = 10$ . The panels are in the same arrangement as in Figure 5.

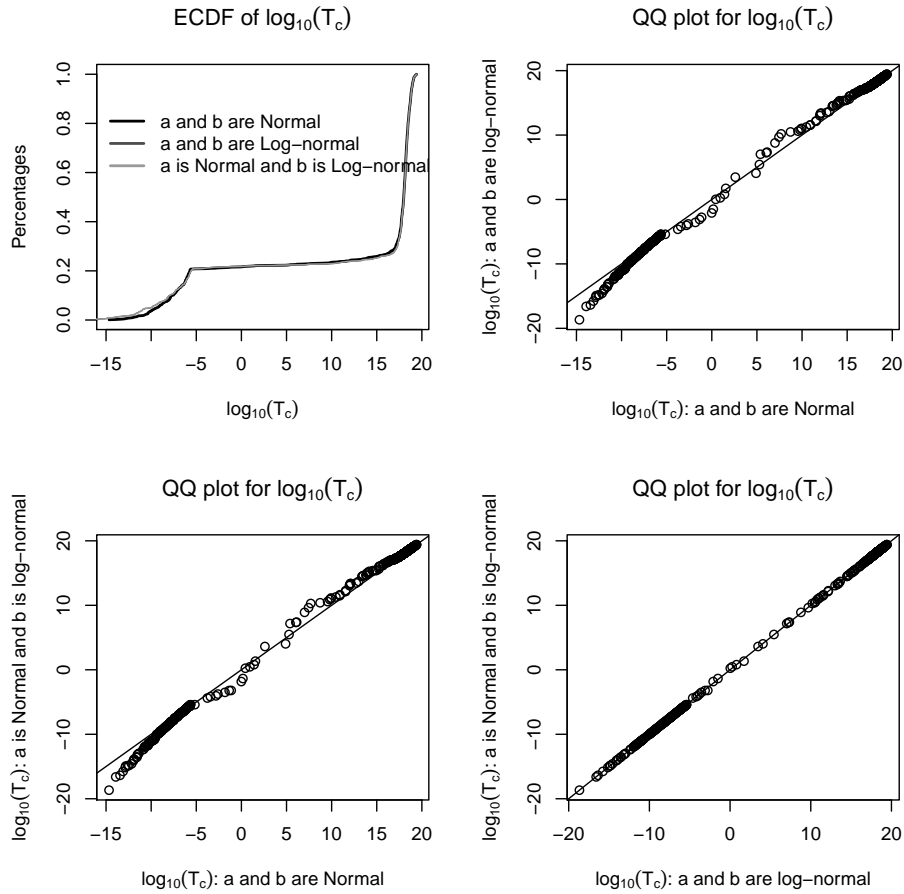


Figure 12: Comparisons of the generated  $T_c$  in the U.S. model based on the three different distributional assumptions of  $a$  and  $b$  when  $\mu_a = 43$ ,  $\mu_b = 50$ ,  $\sigma_a = 1$ ,  $\sigma_b = 10$  and  $p = 0.2$ . The panels are in the same arrangement as in Figure 5.

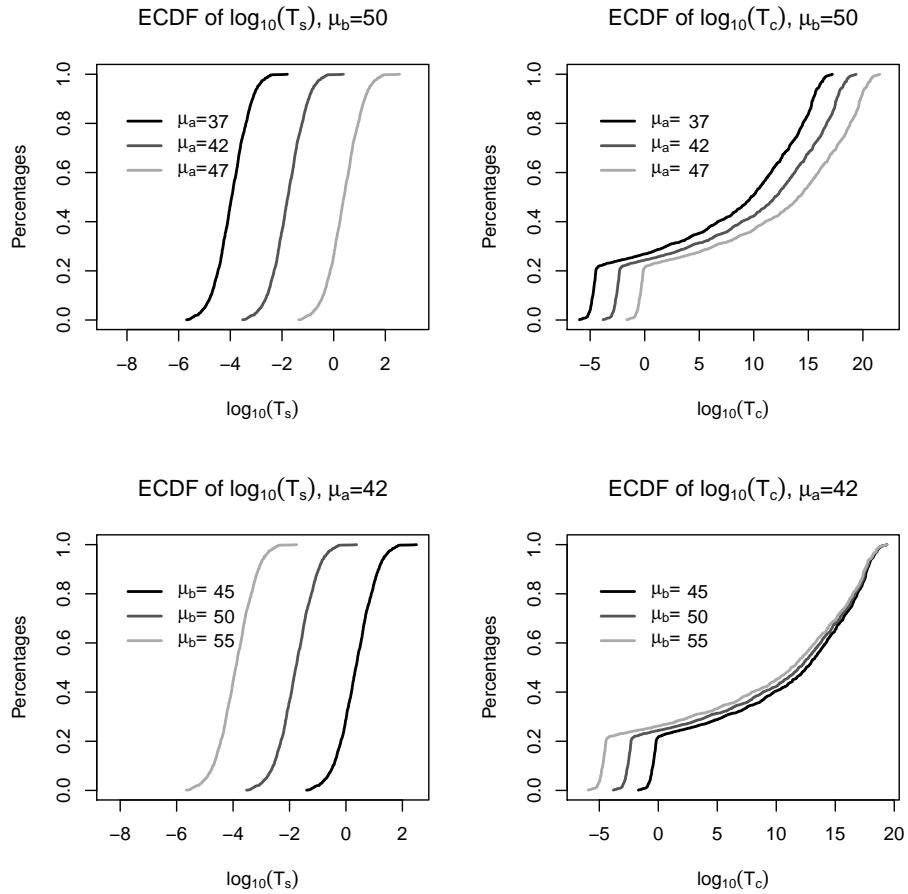


Figure 13: Comparisons of the empirical cumulative distributions of the generated  $T_s$  and  $T_c$  from the U.S. model based the assumption that  $a$  and  $b$  are both Normal,  $\sigma_a = 1$  and  $\sigma_b = 1$ . One mean is fixed at the value stated in the plot title.

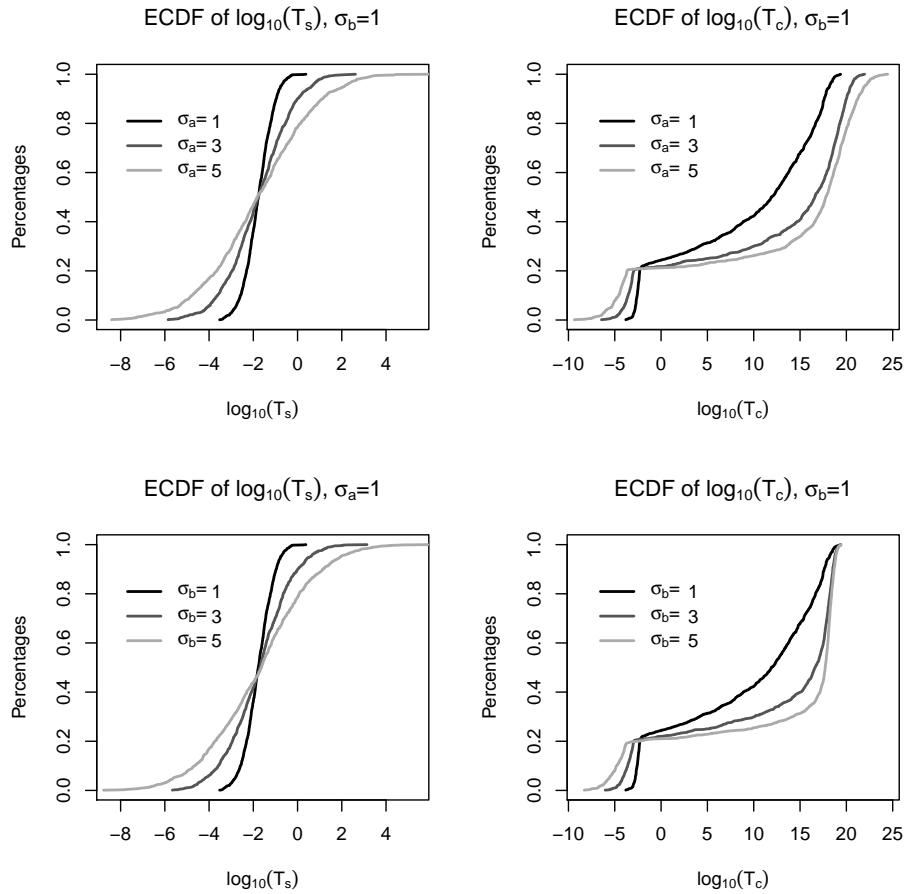


Figure 14: Comparisons of the empirical cumulative distributions of the generated  $T_s$  and  $T_c$  from the U.S. model based the assumption that  $a$  and  $b$  are both Normal,  $\mu_a = 42$  and  $\mu_b = 50$ . One standard variation is fixed at the value stated in the plot title.

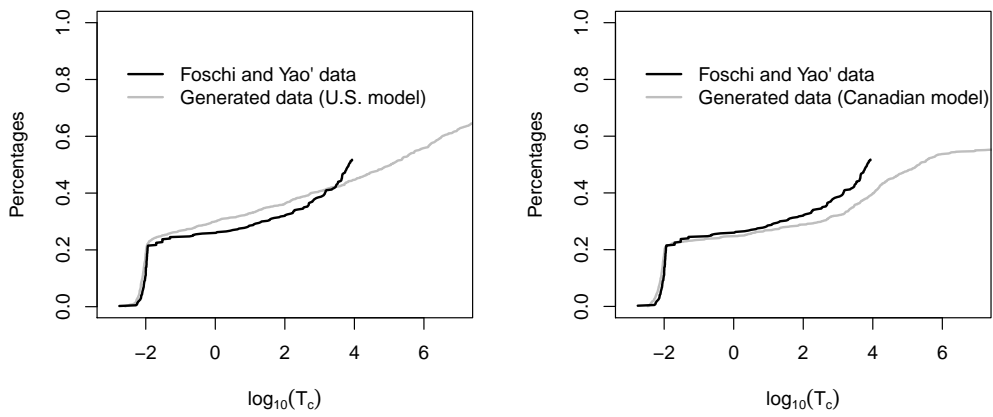


Figure 15: Comparisons of the empirical cumulative distributions of breaking times  $T_c$ 's from Foschi and Yao's experiments and the generated  $T_c$  based on the U.S. model (left panel), and the Canadian model (right panel).

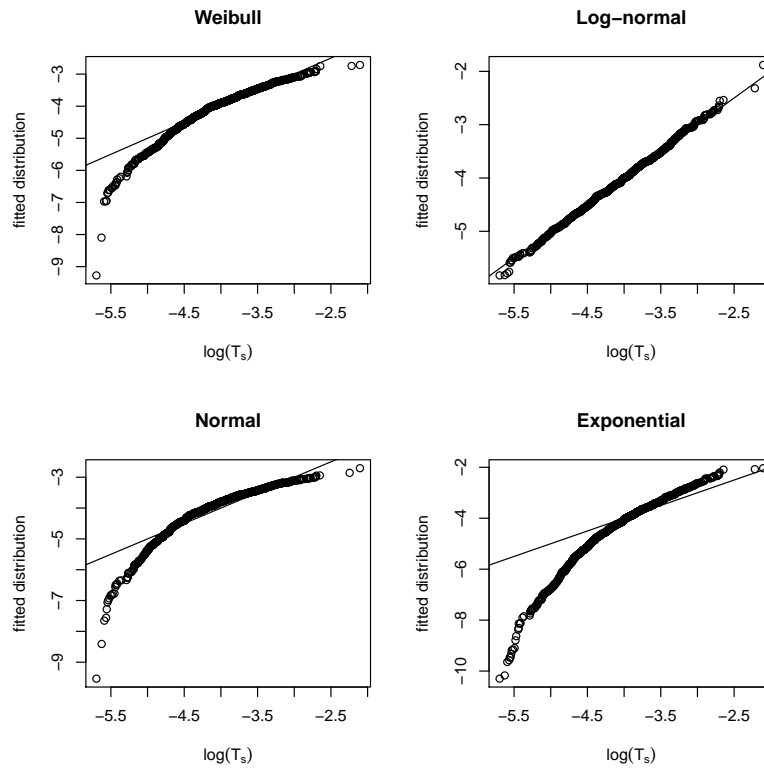


Figure 16: The quantile-quantile plots of the logarithm of the generated breaking times  $T_s$  based on the U.S. model when  $(\mu_a, \mu_b, \sigma_a, \sigma_b) = (42, 50, 0.4, 0.4)$  and the logarithm of simulated data from the fitted distributions. The type of fitted distribution is shown in the title of the plot.

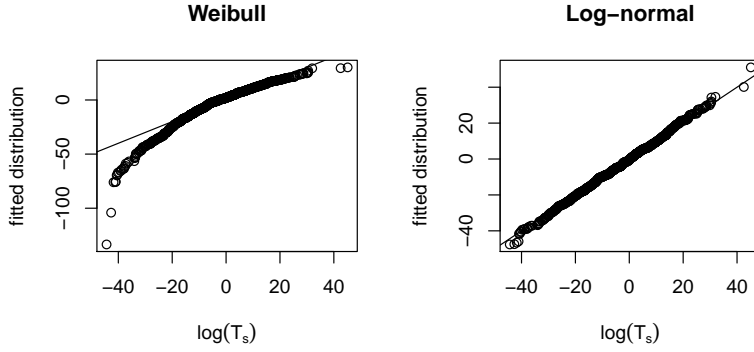


Figure 17: The quantile-quantile plots of the logarithm of the generated breaking times  $T_s$  based on the U.S. model when  $(\mu_a, \mu_b, \sigma_a, \sigma_b) = (42, 50, 10, 10)$  and the logarithm of simulated data from the fitted distributions. The type of fitted distribution is shown in the title of the plot.

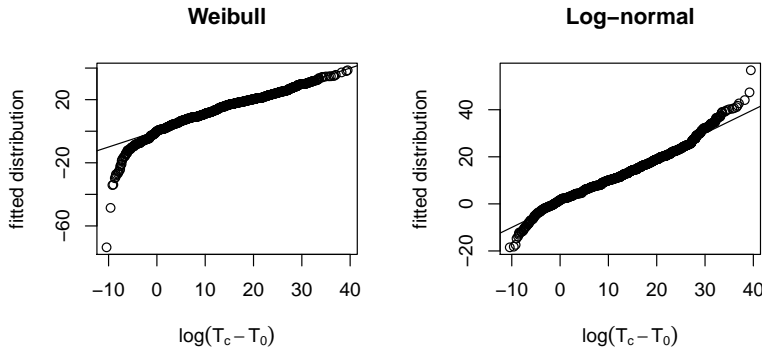


Figure 18: The quantile-quantile plots of the logarithm of the generated breaking times  $T_c$  based on the U.S. model when  $(\mu_a, \mu_b, \sigma_a, \sigma_b) = (42, 50, 0.4, 0.4)$  and  $p = 0.2$ , and the logarithm of simulated data from the fitted distributions. The fitted distribution is shown in the title of the plot.

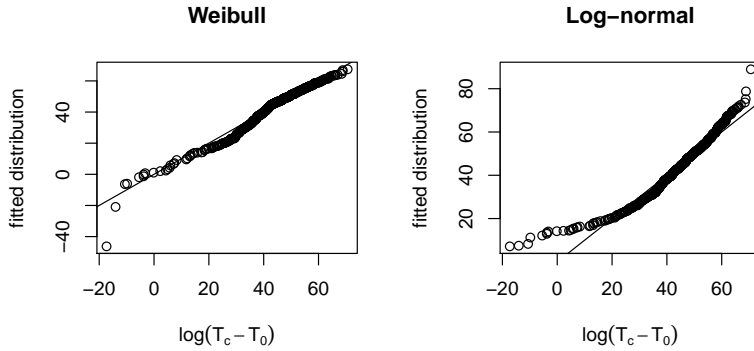


Figure 19: The quantile-quantile plots of the logarithm of the generated breaking times  $T_c$  based on the U.S. model when  $(\mu_a, \mu_b, \sigma_a, \sigma_b) = (42, 50, 10, 10)$  and  $p = 0.2$ , and the logarithm of simulated data from the fitted distributions. The type of fitted distribution is shown in the title of the plot.

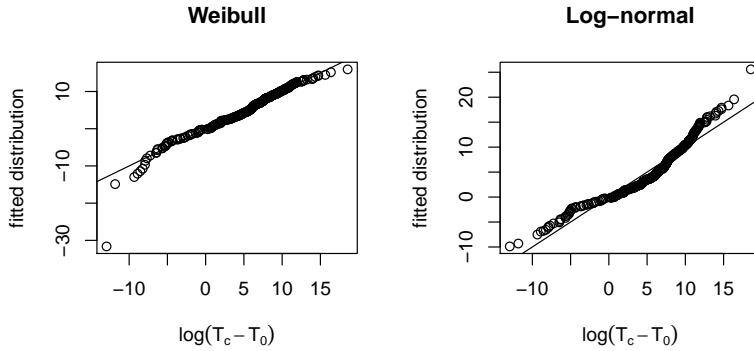


Figure 20: The quantile-quantile plots of the logarithm of the generated breaking times  $T_c$  based on the Canadian model and the logarithm of simulated data from the fitted distributions. The type of fitted distribution is shown in the title of the plot.